Title	Evidence for the involvement of branchial Vacuolar-type H+-ATPase in the acidification of the external medium by the West African lungfish, Protopterus annectens, exposed to ammonia-loading conditions
Author(s)	Yuen K. Ip, Charmaine W. Q. Leong, Mel V. Boo, Wai P. Wong, Siew H. Lam and Shit F. Chew

The final publication is available at: https://doi.org/10.1016/j.cbpa.2022.111297

Evidence for the involvement of branchial Vacuolar-type H^+-ATPase in the acidification of the external medium by the West African lungfish, *Protopterus annectens*, exposed to ammonia-loading conditions

Yuen K. Ip[1*], Charmaine W. Q. Leong[1], Mel V. Boo[1], Wai P. Wong[1], Siew H. Lam[1], and Shit F. Chew[2]

[1]Department of Biological Sciences, National University of Singapore, Kent Ridge, Singapore 117543, Republic of Singapore

[2]Natural Sciences and Science Education, National Institute of Education, Nanyang Technological University, 1 Nanyang Walk, Singapore 637616, Republic of Singapore

*author for correspondence

Running head: Vha and ammonia defence in *P. annectens*

Correspondence address:
Dr. Y. K. Ip
Professor
Department of Biological Sciences
National University of Singapore
Kent Ridge
Singapore 117543
Republic of Singapore

Phone: (65)-6516-2702
Fax: (65)-6779-2486
Email: dbsipyk@nus.edu.sg

Abstract

African lungfishes are obligatory air-breathers with exceptionally high environmental ammonia tolerance. They can lower the pH of the external medium during exposure to ammonia-loading conditions. This study aimed to demonstrate the possible involvement of branchial vacuolar-type H^+-ATPase (Vha) in the ammonia-induced acidification of the external medium by the West African lungfish, *Protopterus annectens*, and to examine whether its capacity to acidify the medium could be augmented after exposure to 100 mmol l^{-1} NH_4Cl for six days. Two full coding cDNA sequences of *Vha subunit B* (*atp6v1b*), *atp6v1b1* and *atp6v1b2*, were obtained from the internal gills of *P. annectens*. The sequence of *atp6v1b1* comprised 1548 bp, encoding 515 amino acids (57.4 kDa), while that of *atp6v1b2* comprised 1536 bp, encoding 511 amino acids (56.6 kDa). Using a custom-made antibody reactive to both isoforms, immunofluorescence microscopy revealed the collective localization of Atp6v1b (atp6v1b1 and atp6v1b2) at the apical or the basolateral membrane of two different types of branchial Na^+/K^+-ATPase-immunoreactive ionocyte. The ionocytes labelled apically with Atp6v1b presumably expressed Atp6v1b1 containing a PDZ-binding domain, indicating that the apical Vha was positioned to transport H^+ to the external medium. The expression of Atp6v1b was regulated post-transcriptionally, as the protein abundance of Atp6v1b and Vha activity increased significantly in the gills of fish exposed to 100 mmol l^{-1} NH_4Cl for six days. Correspondingly, the fish exposed to ammonia had a greater capacity to acidify the external medium, presumably to decrease the ratio of $[NH_3]$ to $[NH_4^+]$ in order to reduce the influx of exogenous NH_3.

Keywords: Acidification, air-breathing fishes, nitrogen metabolism, pH, proton ATPase, urea

1. Introduction

Lungfishes (class Sarcopterygii, subclass Dipnoi) are an archaic group of air-breathing freshwater fishes that possess primitive lungs (Graham, 1997). There are six species of extant lungfishes belonging to families Protopteridae, Lepidosirenidae and Ceratodontidae located in Africa, South America and Australia, respectively. Protopteridae comprises four species of African lungfishes, which possess a functional ornithine-urea cycle in the liver (Chew et al., 2003b; Loong et al., 2005). Despite being ureogenic, African lungfishes are ammonotelic in water and only shift to ureotely transiently after feeding (Chew et al., 2003b; Lim et al., 2004). They can survive on land for an extended period and estivate inside dried mucous cocoons in mud for 4-5 years during drought (Fishman et al., 1986; Chew et al., 2015).

Ammonia is a toxic nitrogenous waste and needs to be excreted (Chew et al., 2006; Chew and Ip, 2014, 2017; Ip and Chew, 2010, 2018). Aquatic fishes generally excrete ammonia as NH_3 through their gills down a favourable blood-to-water diffusive P_{NH3} gradient (Wilkie, 1997; Evans et al., 2005; Weihrauch et al., 2009). When exposed to terrestrial conditions, the excreted ammonia could build-up in the unstirred-layer of water covering the branchial and cutaneous surfaces, impeding ammonia excretion and leading to the accumulation of endogenous ammonia. Hence, African lungfishes need to defend against ammonia toxicity on land due to the impediment of ammonia excretion. Decreased ammonia production and increased urea synthesis are important strategies adopted by African lungfishes to prevent the accumulation of internal ammonia to deleterious levels during terrestrial exposure or estivation (Ip et al., 2001, 2004a, b; Loong et al., 2005; Chew et al., 2006). When trapped in mud puddles preceding complete desiccation during drought, ammonia can build up in the external medium due to the continuous excretion of ammonia by the lungfish as well as the biodegradation of organic matters and evaporation. Ammonia may also accumulate inside the breeding nest for similar reasons (Brien et al., 1959), although the exact environmental ammonia concentrations

remain unknown. Nevertheless, when the environmental ammonia increases to levels that could reverse the blood-to-water P_{NH3} gradient, a net influx of exogenous ammonia into the fish (ammonia-loading) would occur.

In water, ammonia exists as molecular NH_3 and ionic NH_4^+, which can interconvert according to the reaction $NH_3 + H_3O^+ \rightleftharpoons NH_4^+ + H_2O$ with a pK of 9.0 - 9.5 (Whitfield, 1974). Accordingly, the excretion of proton (H^+) by the fish can augment ammonia excretion through trapping the excreted NH_3 as NH_4^+ in the boundary water layer covering the branchial epithelium (Shih et al., 2008; Liu et al., 2013). In the case of ammonia-loading, increased acid excretion can decrease the ratio of environmental NH_3 to NH_4^+ and reduce the net influx of exogenous NH_3 (Chew et al., 2003a; see Ip and Chew 2010, 2018; Chew et al., 2015; Chew and Ip 2014, 2017 for reviews). African lungfishes have remarkably high tolerance of environmental ammonia, which is attributable to their abilities to detoxify ammonia through increased ureogenesis (Chew et al., 2005; Loong et al., 2007, 2012), reduce the ammonia permeability of the body surfaces (Loong et al., 2007), and lower the pH of the bulk of the external medium containing ammonia (Wood et al., 2005). Wood et al. (2005) reported that the slender lungfish, *Protopterus dolloi*, could greatly acidify (from ~ pH 7.0 to ~ pH 5.0) the external medium that contained 30 mmol l^{-1} NH_4Cl in a volume 25-fold greater than the mass of the fish, and proposed that vacuolar-type H^+-ATPase (Vha) could be involved in the acidification process.

VHA/Vha transports H^+ electrogenically out of the cytoplasm against the H^+ concentration gradient using the energy released from ATP hydrolysis (Mindell, 2012) with a proposed stoichiometric ratio of 2 H^+ transported per ATP hydrolysed (Tomashek and Brusilow, 2000). It consists of a cytoplasmic/catalytic V_1 domain and a transmembrane V_0 domain. The V_1 domain consists of subunits A and B, which make up the catalytic headpiece involved in ATP hydrolysis (Forgac, 2000). Subunit B has two isoforms: the kidney isoform (ATP6V1B1) found usually in renal cells, and the brain isoform (ATP6V1B2) that is expressed ubiquitously

in many cell types (Nelson et al., 1992; van Hille et al., 1994). Vha is expressed in the branchial epithelium of freshwater fishes (Lin et al., 1994), and can be involved in osmoregulation (Perry et al., 2003; Kirschner, 2004) as well as acclimation to hypercapnia or hyperoxia (Seidelin et al., 2001). In the gills of freshwater fishes, the excretion of H^+ through the apical Vha can generate an electrochemical gradient to drive the uptake of exogenous Na^+ in certain type of ionocyte (Lin and Randall, 1991; Wilson et al., 2000a; see reviews by Hwang and Lee, 2007; Hwang et al., 2011). Vha can also promote branchial ammonia excretion through boundary layer acidification, trapping the excreted NH_3 as NH_4^+ in the boundary layer (Nawata et al., 2007; Shih et al., 2008).

The West African lungfish, *Protopterus annectens*, can survive exposure to ammonia-loading conditions (100 mmol l^{-1} NH_4Cl at pH 7.0) for at least six days (Chew et al., 2005; Loong et al., 2012). While it is uncertain whether African lungfishes would encounter concentrations of ammonia as high as 30 – 100 mmol l^{-1} in their natural habitat, our intention was to exploit these ammonia-loading conditions to elucidate the possible relationship between branchial Vha and ability of these lungfishes to acidify the external medium containing ammonia. Therefore, this study was conducted to clone *Vha subunit B* isoforms (*atp6v1b1* and *atp6v1b2*) from the internal gills (referred to as gills hereafter) of *P. annectens*. The gene expression levels of *atp6v1b1* and *atp6v1b2* in different organs of *P. annectens* were examined to test the hypothesis that they were expressed strongly in the gills. While specific primers were designed to determine the transcript levels of *atp6v1b1* and *atp6v1b2* through quantitative real-time polymerase chain reaction (qPCR), a comprehensive anti-Atp6v1b antibody was custom-made to determine the cellular localization of Atp6v1b1 and Atp6v1b2 collectively through immunofluorescence microscopy due to high sequence similarity. Furthermore, the transcript levels of *atp6v1b1*/*atp6v1b2*, the protein abundance of Atp6v1b, and the activity of Vha in the gills of individuals of *P. annectens* kept in fresh water (control) and individuals exposed to ammonia-loading conditions (100 mmol l^{-1} NH_4Cl at pH 7.0) were determined. The hypothesis

129 tested was that ammonia-loading could lead to increases in the expression level and activity of
130 Vha. Finally, efforts were made to examine whether exposure of individuals to ammonia-
131 loading conditions for six days would enhance their capacity to lower the pH of the ammonia-
132 containing external medium in accordance with the increase in branchial Vha activity.
133

2. Materials and methods

2.1. Animals

Protopterus annectens specimens (80 - 150 g; total n = 35) were imported from Central Africa through a Singaporean fish farm (Qian Hu Fish Farm Trading Co, Singapore). The current IUCN Red List status of *P. annectens* is Least Concern (IUCN, 2021). All procedures in this study were conducted with the approval of the Institutional Animal Care and Use Committee (IACUC) of the National University of Singapore (NUS) according to the protocol IACUC 035/09. Fish were kept in individual plastic aquaria (L 29 × W 19 × H 17.5 cm) in 2 l of dechlorinated tap water (~pH 7.2) supplemented with seawater to Salinity 2 (referred to as fresh water hereafter) and maintained at 25 °C as described in Wood et al. (2005). The water contained 30 mmol·l^{-1} Na^+, 35 mmol·l^{-1} Cl^-, 3.5 mmol·l^{-1} Mg^{2+}, 2.5 mmol·l^{-1} Ca^{2+}, 2.6, and the titration alkalinity to pH 4.0 was 0.67 mmol·l^{-1}. These fish were acclimated to the laboratory conditions for two weeks, with daily changing of water and feeding with frozen bloodworms. Feeding was withheld 48 h before the start of the experiment.

2.2. Experimental conditions and collection of tissue samples

After pre-acclimatisation, twenty individuals of *P. annectens* were split into four groups for sampling of tissues for molecular work. Fish (n = 5) sampled after the acclimatisation stage without exposure to NH_4Cl constituted the control group. The remaining three groups (n = 5 each) were immersed in water containing 100 mmol l^{-1} NH_4Cl at pH 7.0 with aeration for 1, 3 or 6 days with daily water changes before killing by an overdose of neutralised MS222 (0.05%). All the gill arches from the right and left opercular cavities were excised quickly from each individual along with tissues from other organs (gills, gut, kidney, liver, lung, muscle, pancreas, skin and spleen,). Samples were immediately freeze-clamped with precooled aluminium tongs and stored at -80 °C until analysis.

158 In addition, four control fish (n = 4) and four fish that had been exposed to 100 mmol l^{-1}
159 NH_4Cl at pH 7.0 with aeration for six days (n = 4) were killed for the sampling of gills for
160 Vha assays. Gill samples were blotted dry and immediately freeze-clamped with liquid-
161 nitrogen-precooled aluminum tongs and immersed in 1 ml of solution containing 100 mmol l^{-1}
162 imidazole-HCl buffer (pH 7.1), 300 mmol l^{-1} sucrose, 20 mmol l^{-1} EDTA (Zaugg, 1982) before
163 storage at -80 ˚C. Samples were assayed for Vha activity within one month of collection.
164 For immunofluorescence microscopy, gill samples were collected from three fish (n =
165 =3) kept in the control condition and fixed in 4% paraformaldehyde in phosphate buffered
166 saline (PBS) overnight at 4 °C.
167 ***2.3. Total RNA extraction and cDNA synthesis***
168 Samples were pounded with a mortar and pestle. Then, the total RNA of a sample was extracted
169 by homogenisation in TRI Reagent™ (Sigma-Aldrich, St. Louis, MO, USA) using a 1600
170 MiniG® tissue homogeniser and cell lyser (SPEX SamplePrep, Metuchen, NJ, USA) with 2.8
171 mm metal beads for 2 min at 1500 strokes min^{-1}. RNA purification was performed using the
172 RNeasy Plus Mini Kit (Qiagen, Hilden, Germany). RNA was quantified using a Shimadzu
173 BioSpec-nano spectrophotometer (Shimadzu, Tokyo, Japan) and RNA integrity was evaluated
174 by gel electrophoresis. The purified RNA (2 μg) was reverse transcribed into first-strand cDNA
175 synthesis using a RevertAid™ First Strand cDNA synthesis kit (Thermo Fisher Scientific Inc.,
176 Waltham, MA, USA).
177 ***2.4. PCR and RACE-PCR***
178 The partial sequences of *atp6v1b* were obtained using a set of polymerase chain reaction (PCR)
179 primers (forward: 5'-CDGTRTCHGAGGACATGCTGGG-3'; reverse: 5'-
180 RATRGGGATYTGWGTGATRGAG-3'). This set of primer was designed based on the
181 homologous regions found in various *atp6v1b* sequences of fish and amphibian *atp6v1b*
182 sequences. These sequences included *Lepisosteus oculatus atp6v1b1 isoform X2*
183 (XM_015343799.1), *Xenopus tropicalis atp6v1b1* (NM_001114262.1), *Nanorana parkeri*

184 *atp6v1b1* (XM_018560470.1), *Periophthalmodon schlosseri vatb2* (KT946763.1), *Nanorana*
185 *parkeri atp6v1b2* (XM_018566204.1), *Xenopus tropicalis atp6v1b2* (NM_001078714.2),
186 *Oryzias latipes atp6v1ba* (NM_001278849.1), *Esox lucius atp6v1b2* (XM_010892252.4) and
187 *Astyanax mexicanus atp6v1b2* (XM_007229909.3).

188 PCR was performed using in a 9902 Veriti 96-well thermal cycler (Applied Biosystems,
189 Carlsbad, CA, USA) and DreamTaq™ polymerase (Thermo Fisher Scientific Inc.). The PCR
190 cycling conditions were as follows: initial denaturation at 95 °C (3 min), followed by 40 cycles
191 of denaturation, annealing and extension at 95 °C (30 s), 60 °C (30 s) and 72 °C (1 min),
192 respectively, as well as a final extension at 72 °C for 10 min. The PCR products were separated
193 by electrophoresis in 1% agarose gel. Bands at the estimated molecular mass of 700 bp were
194 excised and purified using the Wizard® SV Gel and PCR clean-up system (Promega
195 Corporation, Madison, WI, USA).

196 The purified PCR products were cloned into pGEM®-T Easy vectors (Promega
197 Corporation, Madison, WI, USA) and transformed into JM109 competent cells by heat-shock,
198 before being plated on Luria Bertani (LB) agar with ampicillin, X-gal and IPTG. White colonies
199 were grown in ampicillin-containing LB broth and colony PCR was done using with primers
200 T7 and SP6 to verify that the correct vector was taken up. Plasmids were extracted and purified
201 using the plasmid miniprep kit (Axygen Biosciences, Union City, CA, USA). The bidirectional
202 sequencing was done using BigDye® Terminator v3.1 Cycle Sequencing Kit (Applied
203 Biosystems) with a 3130XL Genetic Analyzer (Thermo Fisher Scientific Inc.). BioEdit version
204 7.2.5. (Hall 1999) was used to view and analyse the sequences, in order to identify *atp6v1b1*
205 and *atp6v1b2* through analysis using the database in National Center for Biotechnology
206 Information (https://blast.ncbi.nlm.nih.gov/Blast.cgi).

207 RACE-PCR using the SMARTer™ RACE cDNA amplification kit (Clontech
208 Laboratories, Mountain View, CA, USA) and gene-specific primer sets was performed to
209 obtain the full cDNA sequences of *atp6v1b1* and *atp6v1b2*. For *atp6v1b1*, the 5' and 3' RACE

primers were 5'-AACTCCTCGTCTTGCTCTAACTACAGC-3' and 5'-GGCCATCCATTGTTCCTTTATGCT-3', respectively. For *atp6v1b2*, the 5' and 3' RACE primers were 5'-TTGGCCTTGACAGCGGCAGAGTTT-3' and 5'-TCATGCCATCTATAGCAGAGATCCCGGT-3', respectively.

2.5. Deduced amino acid sequences and phenogramic analyses

The nucleotide sequences of *atp6v1b1* and *atp6v1b2* were translated into Atp6v1b1 and Atp6v1b2 amino acid sequences using ExPASy Proteomic server (http://web.expasy.org/translate/). Transmembrane (TM) regions were predicted using TOPCONS consensus prediction server (http://topcons.cbr.su.se/) (Tsirigos et al., 2015).

BioEdit was used to align the Atp6v1b1 and Atp6v1b2 amino acid sequences of *P. annectens* with Atp6v1b sequences of selected animal species obtained from GenBank for comparison. Phenogramic analysis was performed using RaxML v8.2.5 (Stamatakis, 2014) through the maximum-likelihood analysis with 4000 bootstraps on selected amino acid sequences from GenBank for other animal species (Supplementary Table S1). The trees converged after 2600 bootstraps by the bootstrap convergence criterion. JTT + I + G (Jones et al., 1992) was regarded as the best-fitting evolutionary model under the Akaike Information Criterion using the ModelGenerator v0.85 (Keane et al., 2006).

2.6. Quantitative real-time PCR (qPCR)

cDNA (2 μg) of was synthesized as mentioned above using random hexamer primers. Specific primers for quantitative real-time PCR (qPCR) were designed based on full cDNA sequences obtained for *atp6v1b1* (forward: 5'-CATAAAGGAACAATGGATGG-3'; reverse: 5'-AGGATCATTTGCCAGGTTTA-3') and *atp6v1b2* (forward: 5'-TTAACGGAGCGATGAATGA-3'; reverse: 5'-CATTGACACCCGAGACAGT-3'). The absolute quantification method was adopted to determine the transcript levels of *atp6v1b1* and *atp6v1b2*, and results were expressed as absolute copies of transcript per ng of total RNA.

qPCR was performed in triplicates in a 10 µl reaction using the reagent qPCRBIO SyGreen Mix Hi-ROX (PCR Biosystems Inc., Wayne, PA, USA). The StepOnePlus™ Real-Time PCR System (Applied Biosystems) was used with cycling conditions of one cycle of 95 °C (20 s), followed by 40 cycles of 95 °C (3 s) and 62 °C (30 s). A melt curve analysis was included to verify the purity of the product by confirming the presence of only one product. The threshold cycle (C_t) values, C_t slope, efficiency, correlation coefficient (r^2) and y-intercept were generated using the StepOne Software v2.3. The qPCR products were separated on a 2% agarose gel, and sequenced to ensure the correct sequence was obtained. The absolute quantity of transcripts was calculated from a plasmid standard curve generated according to the method of Chew et al. (2014).

2.7. Antibodies

It was not feasible to generate two antibodies that could differentiate Atp6v1b1 and Atp6v1b2 due to the high similarity between these two sequences. Therefore, a custom-made rabbit polyclonal antibody that would react comprehensively with Atp6v1b1 and Atp6v1b2, denoted Atp6v1b, was produced by a commercial firm (GenScript, Piscataway, NJ, USA), and used for immunofluorescence microscopy as well as immunoblotting. The epitope sequence used to generate the anti-Atp6v1b antibody was NGSGKPIDRGPSVL, which shared 11/14 residues with Atp6v1b1 (residues 128 to 141) and 13/14 residues with Atp6v1b2 (residues 132 to 145). α-Tubulin was chosen as the reference protein for western blotting and the anti-α-tubulin antibody (12G10, 0.1 µg ml^{-1}) was obtained from the Developmental Studies Hybridoma Bank (Department of Biological Sciences, University of Iowa, Iowa City, USA). The anti-NKAαRb1 mouse polyclonal antibody, which is a pan-specific antibody originally designed by Ura et al. (1996) to label Nka α-subunit isoforms, was custom-made by GenScript.

2.8. Immunofluorescence microscopy

Gill sections were decalcified, dehydrated in graded ethanol, cleared in Histochoice Clearing Agent (Sigma), embedded in Paraplast (Sigma) and sliced into 3 µm sections. Antigen retrieval

was performed by boiling in 0.05% citraconic anhydride (Nacalai Tesque Inc., Kyoto, Japan) for 15 min. Sections were then placed in permeabilizing solution of 1% sodium dodecyl sulfate in PBS-T (0.05% Tween 20 in PBS; pH 7.4) for 10 min at room temperature. Blocking of non-specific binding was achieved by immersing sections in 1% bovine serum albumin in PBS-T for 30 min. The sections were incubated for 1 h at 25 ºC in the rabbit polyclonal anti-Atp6v1b antibody (2.5 mg ml^{-1}) and the mouse polyclonal anti-NKAαRb1 antibody (1.67 mg ml^{-1}). These primary antibodies were diluted in Immunostain Solution A of the Signal Enhancer HIKARI kit (Nacalai Tesque Inc.). Then, the sections were incubated for 1 h at 25 ºC with the goat anti-mouse Alexa Fluor® 568 and the goat anti-rabbit Alexa Fluor® 488 (2 mg ml^{-1} dilution; Life Technologies Inc.) in Immunostain Solution B of the Signal Enhancer HIKARI kit. They were rinsed with PBS-T, followed with mounting on glass slides using Prolong Gold Antifade reagent (Thermo Fisher Scientific Inc.). Stained samples were viewed under an epifluorescence microscope (Olympus BX60, Olympus Corporation., Tokyo, Japan) equipped with the necessary filters. Tissue structure of the gills was examined by differential interference contrast (DIC) microscopy. Images were captured with a CCD camera and merged using Adobe Photoshop CC (Adobe Systems, San Jose, CA, USA), with uniformly adjusted brightness and contrast.

2.9. Sodium dodecyl sulfate-polyacrylamide gel electrophoresis (SDS-PAGE) and western blotting

Proteins were extracted from the gill samples by homogenizing for 2 min at 1500 strokes min^{-1} with metal beads in five volumes (w/v) of ice-cold buffer. The buffer consisted of 50 mmol l^{-1} of Tris HCl (pH 7.4), 150 mmol l^{-1} NaCl, 1 mmol l^{-1} ethylenediaminetetraacetic acid (EDTA), 1 mmol l^{-1} NaF, 1 mmol l^{-1} Na_3VO_4, 1 mmol l^{-1} PMSF, 1% NP-40, 1% sodium deoxycholate, and 1 × HALT™ protease inhibitor cocktail (Thermo Fisher Scientific Inc.). The supernatant was collected after centrifugation at 12,000 × *g* for 15 min at 4 °C. Protein concentrations of the supernatants were determined using the method of Bradford (1976) with bovine γ-globulin

as a standard for comparison. Laemmli buffer (Laemmli, 1970) was used to adjust the protein concentrations to 10 μg μl^{-1} before storing them at -80 °C.

Protein samples (25 μg) were separated through SDS-PAGE electrophoresis (4% acrylamide in stacking gel, 8% acrylamide in resolving gel) using the vertical mini-slab apparatus (Bio-Rad Laboratories, Hercules, CA, USA). Separated proteins were transferred from the gel to a nitrocellulose membrane using a transfer apparatus (Bio-Rad Laboratories). All reagents used for chemiluminescence and for antibody dilution were from the Pierce Fast Western Blot kit (Thermo Fisher Scientific Inc.). After fixing with 60% methanol, the membrane was blocked for 10 min using SuperBlock™ blocking buffer (Thermofisher Scientific Inc.). It was then incubated with the anti-Atp6v1b antibody (0.286 μg ml^{-1}) at 25 ºC for 1 h, followed with anti-rabbit or anti-mouse (for tubulin) horseradish peroxidase-conjugated secondary antibodies at 25 °C for 15 min, before washing and further incubation with substrate luminol and hydrogen peroxidase. Chemiluminescence of the relevant protein bands was visualize using the ChemiDoc™ Imaging System (Bio-Rad Laboratories). Quantification of the optical density of the bands was performed using ImageJ (version 1.40, NIH), and calibration of the optical density was conducted using 21-step Tiffen transmission photographic step tablet (EK1523406T; Tiffen Company, Rochester, NY). The relative protein abundance of Atp6v1b was obtained by normalizing the optical density of the Atp6v1b band with that of the tubulin band.

2.10. Determination of Vha activity

Thawed gill samples were washed three times with a buffer, which contained 300 mmol l^{-1} sucrose in 100 mmol l^{-1} imidazole-HCl buffer (pH 7.1). They were then homogenized three times using a Polytron homogenizer at 13,500 rpm for 15 s each with two 10 s intervals in five volumes of buffer containing 300 mmol l^{-1} sucrose and 0.1% of sodium deoxycholate in100 mmol l^{-1} imidazole-HCl buffer (pH 7.1). The homogenized sample was centrifuged at 4,000 x*g* at 4 ºC for 5 min and the supernatant obtained was used for determining the activities of Vha.

Vha activity was determined following the methods of Ip et al. (2015). An aliquot of the supernatant (0.05 ml containing ~0.1 mg protein) was pre-incubated for 10 min at 25 ºC in 1 ml of reaction mixture, which contained 30 mmol l^{-1} imidazole-HCl buffer (pH 7.1), 5 mmol l^{-1} $MgCl_2$, 5 mmol l^{-1} NaN3, 2 mmol l^{-1} ouabain and 20 µl dimethylsulfoxide. A blank was prepared in the same reaction mixture containing a final concentration of 30 µmol l^{-1} bafilomycin A1 (Sigma-Aldrich Co., St, Louis, MO, USA) that was dissolved in 20 µl of dimethylsulfoxide. After 10 min of pre-incubation, 50 µl of 3.5 mmol l^{-1} ATP was added to initiate the reaction, which lasted 40 min at 25 ºC. Preliminary data confirmed that the reaction rate remained constant up to 60 min. At the end of the 40 min of incubation, the reaction was stopped by the addition of 0.05 ml of ice-cold 100% trichloroacetic acid. The resulting mixture was centrifuged for 2 min at 10,000 × *g* and at 4 ºC. The supernatant obtained was used for the determination of the amount of inorganic phosphate (Pi) released from ATP during the reaction. To assay for Pi, an aliquot (0.4 ml) of the supernatant was diluted with 4 vol of 0.1 mol l^{-1} sodium acetate, followed with the addition of 0.2 ml of 1% ammonium molybdate in 0.05 mol l^{-1} H_2SO_4 and 0.2 ml of 1% ascorbic acid. The absorbance was recorded at 700 nm using a Shimadzu (Shimadzu Corp., Kyoto, Japan) UV160 UV-VIS spectrophotometer. Standards made from KH_2PO_4 were used as references for comparison. The ATPase activity of bafilomycin-sensitive-Vha was calculated as the difference in activities between the reactions with and without bafilomycin. Results were expressed as µmol Pi released min^{-1} g^{-1} wet mass of gill tissues or µmol Pi released min^{-1} mg^{-1} gill protein. Protein concentrations of the samples were determined following the method of Bradford (1976).

2.11. Effects of exposure to 100 mmol l^{-1} NH_4Cl on the capacity of P. annectens to lower the pH of the external medium

After the acclimation period, four individuals of *P. annectens* with similar body mass (143 - 150 g; n=4) were selected for this experiment. They were transferred individually to a plastic aquaria (L 29 × W 19 × H 17.5 cm) containing 2 l of dechlorinated water containing 100 mmol

339 l^{-1} NH_4Cl, and the pH was carefully adjusted to 7.0 at the start of the experiment. The ambient
340 water was vigorously aerated to prevent the accumulation of CO_2. On day 1 of exposure to
341 ammonia, the pH of the medium was determined at hours 2, 4, 6, 8 and 12 using an Orion model
342 420A pHmeter (Boston, MA, USA) and a Corning G-P Combo w/RJ Tris-electrode (Halstead,
343 Essex, UK). The lungfish was exposed to ammonia in the same tank for another 12 h without
344 disturbance. After 24 h, the external medium containing 100 mmol l^{-1} NH_4Cl was changed and
345 the pH readjusted to 7.0. The lungfish was exposed to ammonia continuously for six days with
346 daily renewal of the ambient ammonia-containing medium. On day 7, the pH of the medium
347 was determined at hour 2, 4, 6, 8 and 12. Four tanks each containing 2 l of 100 mmol l^{-1} NH_4Cl
348 at pH 7.0 but without fish were set up as blanks to estimate the effects on aeration on the pH of
349 the medium. The blank medium was aerated to the same extent as the medium containing the
350 experimental fish.

351 Total ammonia represents the sum of $[NH_3]$ and $[NH_4^+]$, and the ratio of $[NH_3]$ and
352 $[NH_4^+]$ changes with pH. Hence, the Henderson-Hasselbalch equation was applied to calculate
353 the $[NH_3]$ present in the external medium containing 100 mM of total ammonia as NH_4Cl at
354 each time point based on the measured pH and a pK value of 9.25 (Ip et al., 2001; Chew et al.,
355 2006; Ip and Chew, 2010).

356 ***2.12. Statistical analyses***

357 Results were presented as mean ± standard error (SEM). Statistical analyses were performed
358 using SPSS version 26 (IBM Corporation, Armonk, NY, USA). The data set in Fig. 1 was
359 analysed using repeated measures ANOVA with two within-subjects factors: Day and Time.
360 As the interaction between the two factors was found to be significant, comparison of the means
361 at each time point between Day 0 and Day 6 was performed using the Bonferroni's post-hoc
362 test. Similarly, the means at 0 h and 12 h for each day (Day 0 and Day 6) were also compared.
363 On the other hand, the data set in Fig. 6 was analysed using One-Way ANOVA. Levene's test
364 was used to evaluate the homogeneity of variances within the set of data. When significance

365 was observed, comparison of the means among the different groups were performed using
366 Tukey's post-hoc test (equal variance) or Dunnett's T3 post-hoc test (unequal variance).
367 Differences were regarded as statistically significant when the p-value is < 0.05.
368

3. Results

3.1. Nucleotide and amino acid sequences

Two full cDNA coding sequences of *Vha subunit B*, *atp6v1b1* (Genbank accession: MN124098) and *atp6v1b2* (MN124099), were obtained from the gills of *P. annectens*. The nucleotide sequence of *atp6v1b1* consisted of 1548 bp, and that of *atp6v1b2* comprised 1536 bp, and they encoded for amino acid sequences of 515 residues (57.4 kDa) and 511 residues (56.6 kDa), respectively.

The deduced amino acid sequences of Atp6v1b1 and Atp6v1b2 from *P. annectens* were aligned with those of yeast, fish and bovine sequences obtained from GenBank (Fig. 1). Both sequences lacked transmembrane regions as predicted by TOPCONS. The PGRRGYP motif of Vha B subunit was conserved across all sequences examined (Fig. 1). R395 and F366 (numbered according to the sequence of Atp6v1b1 from *P. annectens*) are important residues involved in the catalytic nucleotide binding sites on subunit A, and they were conserved in the Atp6v1b1 sequences. However, similar to bovine ATP6V1B1, a tyrosine was present at position 370 in Atp6v1b2 of *P. annectens*. While most of the residues contributing to the non-catalytic binding sites on subunit B were conserved across various species, fish sequences had a glutamine residue instead of a serine in VMA2 of yeast or a glutamate in ATP6V1B1 of *Bos Taurus*. This glutamine residue was present as Q166 and Q170 in Atp6v1b1 and Atp6v1b2 of *P. annectens*, respectively (Fig. 1). Although a profilin-like domain at the amino-terminus and a part of the sequence corresponding to the glycine-rich loop on subunit A were conserved across all the sequences, only Atp6v1b1/ATP6V1B1 had the D(S/T)XL motif for binding to PDZ proteins, which can define an apical localization in epithelial cells (Breton et al., 2000; Boesch et al., 2003a).

3.2. Phenogramic analysis and gene expression level in various tissues

393 The identities of Atp6v1b1 and Atp6v1b2 of *P. annectens* were further verified by a
394 phenogramic analysis, whereby they were grouped distinctly with Atp6v1b1/ATP6VB1 and
395 Atp6v1b2/ATP6VB2, respectively (Fig. 2). While Atp6v1b1 from *P. annectens* was grouped
396 closer to those of other fishes, Atp6v1b2 from *P. annectens* was clustered closely with those of
397 reptiles.

398 Transcripts of *atp6v1b2* were detected in many organs (gills, liver, spleen, pancreas,
399 lung, gut, kidney muscle and skin) of *P. annectens*, with the gills having the highest level of
400 gene expression followed by the kidney and gut (Fig. 3). By contrast, the transcript of *atp6v1b1*
401 was detected only in the gills and the kidney, and the expression in the former was apparently
402 higher than that in the latter (Fig. 3). The gene expression levels of *atp6v1b1* in the other organs
403 were very weak (gills) or undetectable (Fig. 3).

404 ***3.3. Immunofluorescent localisation of Atp6v1b in the gills***

405 It is noteworthy that the cellular morphology and anatomy of gills of lungfishes are distinct
406 from those of elasmobranchs and teleosts. The gills of *P. annectens* (Sturla, 2001a, b) and those
407 of the South American lungfish, *Lepidosiren paradoxa* (Wright, 1974), are known to have few
408 short and rod-like filaments that bear lobe-like secondary lamellae. These lamellae are covered
409 with a pseudostratified secondary epithelium comprising 4-7 layers of cells, which is much
410 thicker than those of elasmobranchs and teleosts (Wright, 1974; Sturla, 2001a). Specifically,
411 the lamellae of *P. annectens* consist of two morphologically different types of mitochondria-
412 rich cells that are similar to the α and β ionocytes of freshwater teleosts (Sturla, 2001a).

413 Differential interference contrast (DIC) and immunofluorescent images of the gills of *P.*
414 *annectens* (Fig. 4) obtained from this study corroborated previous reports on the branchial
415 histomorphology of this lungfish (Sturla et al., 2001a, b). Because of the presence of multi-
416 layered branchial epithelial cells, it was essential to use Nka as a marker to identify the
417 ionocytes as well as their basolateral membrane in the gills of *P. annectens*. Nka-labelled (in
418 red) ionocytes were detected in both the surface epithelial layer and the inner layers of epithelial

cells (Fig. 4). The lamellae of *P. annections* were thick and lobe-like and did not have the morphological arrangement to promote the counter-flow of water. Hence, the orientation of the sectioned ionocytes differed from those of typical teleosts, and their basolateral membranes appeared circular rather than the usual 'C' shape. As the anti-NKA antibody labelled the basolateral membrane in red, co-labelling with the green anti-Atp6v1b antibody would produce a yellow color that signified the basolateral localization of Atp6v1b. Our results revealed that not all Nka-immunoreactive cells in the gills of *P. annections* were Atp6v1b-immunoreactive. Nonetheless, the immunolabelling of Atp6v1b indicated the presence of two different types of Nka-labelled ionocytes in the gills, which corroborated the findings of Sturla et al. (2001a). One type of Nka-immunoreactive ionocyte had green apical Atp6v1b labelling while another type displayed yellow basolateral Atp6v1b labelling (Fig. 4). The apical and basolateral immunostaining of Atp6v1b in the gills of *P. annectens* was probably attributed to different molecular characteristics of Atp6v1b1 and Atp6v1b2, resulting in their apical and basolateral localization, respectively (see sections 4.2 and 4.4 of Discussion).

3.4. Effects of exposure to 100 mmol l^{-1} NH_4Cl on transcript levels of atp6v1b1 and atp6v1b2 and protein abundance of Atp6v1b in the gills

Exposure to 100 mmol l^{-1} NH_4Cl for six days led to a significant decrease in the transcript level of *atp6v1b1* in the gills of *P. annectens* on day 6, but it had no significant effect on the transcript level of *atp6v1b2* (Fig. 5).

The protein band detected at ~50 kDa on the immunoblot (Figure 6A) was regarded as the Atp6v1b protein because the deduced molecular masses of Atp6v1b1 and Atp6v1b2 ranged between 56 and 58 kDa. After six days of exposure to 100 mmol l^{-1} NH_4Cl, the protein abundance of Atp6v1b increased significantly (~ 3-fold) in the gills of *P. annectens* as compared to the control kept in freshwater (Fig. 6B).

3.5. Effects of exposure to 100 mmol l^{-1} NH_4Cl on the activity of Vha in the gills

444 The activity (μmol Pi released min^{-1} g^{-1} wet mass tissue or μmol Pi released min^{-1} mg^{-1} protein)
445 of bafilomycin-sensitive-Vha from the gills of *P. annectens* kept in water without NH_4Cl
446 (control) increased significantly by ~ 2-fold after six days of exposure to 100 mmol l^{-1} NH_4Cl
447 (Fig. 7).

448 ***3.6. Effects of exposure to 100 mmol l^{-1} NH_4Cl for six days on the capacity of P. annectens***
449 ***to lower the pH of the external medium***

450 Without prior exposure to ammonia, *P. annectens* could reduce the pH of the medium
451 containing 100 mmol l^{-1} NH_4Cl significantly from pH 7.0 to pH 5.8 within a 12-h period (Fig.
452 8A). After exposure to ammonia for six days, there was an increase in the capacity of *P.*
453 *annectens* to lower the pH of the medium containing 100 mmol l^{-1} NH_4Cl. The pH measured at
454 various time points (hour 2, 4, 6, 8 and 12) were significantly lower than the corresponding pH
455 obtained for individuals that had no prior exposure to ammonia. Based on the Henderson-
456 Hasselbalch equation, an estimation of the concentration of NH_3 in the external medium
457 containing 100 mM of total ammonia revealed that the [NH_3] decreased drastically with the
458 marked decrease in ambient pH (Fig. 9). At hour 12, the acidification of the medium (to pH 5.8;
459 Fig. 8) by those individuals without prior exposure to ammonia led to ~ 94% reduction in the
460 concentration of NH_3 in the medium as compared with that at hour 0 (Fig. 9). For individuals
461 that had been exposed to ammonia for six days, there was a ~ 99% reduction in the
462 concentration of environmental NH_3 as compared with the hour 0 value (Fig. 9) because the
463 ambient pH was lowered further to 5.04 (Fig. 8).
464

4. Discussion

4.1. Relationships between H^+ excretion through Vha and ammonia excretion in fish gills

Results from this study support the proposition that branchial Vha could be involved in ammonia-induced acidification of the external medium in *P. annectens*, as exposure to 100 mmol l^{-1} NH_4Cl for six days augmented the protein abundance of Atp6v1b and the activity of Vha in the gills. This might explain why individuals exposed to ammonia for six days displayed a greater capacity to acidify the ammonia-containing medium presumably to reduce the concentration of NH_3 and to lower the toxicity of environmental ammonia (Chew et al., 2003a; Wood et al., 2005). Of note, the giant mudskipper, *Periophthalmodon schlosseri*, can also survive exposure to 100 mmol l^{-1} NH_4Cl. It can actively excrete ammonia against inwardly directed P_{NH3} and NH_4^+ gradients through its gills (Randall et al., 1999; Chew et al., 2007). However, there is no indication that African lungfishes can do the same possibly because of their ability to detoxify ammonia through increased urea synthesis. In *P. schlosseri*, active ammonia excretion occurs through the gills in association with increased branchial H^+ excretion through Vha, which traps the excreted ammonia as NH_4^+ in the external medium to prevent a back flux of NH_3 (Ip et al., 2004c; Chew et al., 2007; Chew and Ip, 2017). It has been reported that *P. schlosseri* can alter the pH of the medium inside an artificial burrow while actively excrete ammonia into it (Ip et al., 2004c; Chew and Ip, 2017).

Although the gills of African lungfishes appear to be morphologically degenerate, they act as an important organ for respiration, ammonia excretion and iono-regulation (McMahon, 1970; Sturla et al., 2001a; Wilkie et al., 2007; Chng et al., 2016, 2017). While oxygen uptake occurs mainly in the lungs of African lungfishes, CO_2 is excreted predominantly through the gills (Lenfant and Johansen 1968; McMahon, 1970; Burggren and Johansen 1986). Wood et al. (2005) reported that vigorous aeration reduced but did not eliminate the ammonia-induced acidification of the external medium by *P. dolloi* indicating that CO_2 excretion was only

partially responsible for the acidification process. The rate of ammonia-induced titratable acid excretion in *P. dolloi* was estimated as ~ 200 μmol·kg^{-1}·h^{-1} and was comparable between the aerated and non-aerated treatments (Wood et al., 2005). Our results demonstrate for the first time that the presence of a type of Nka-immunoreactive ionocyte, which expressed Atp6v1b (probably Atp6v1b1) at the apical membrane, in the gills of *P. annectens*. As VHA/Vha expressed in the plasma membrane is known to facilitate the efflux of H^+ from the cell, it is probable that H^+ could be excreted through this type of branchial ionocyte with apical Atp6v1b expression.

4.2. Molecular characterisation of Atp6v1b1 and Atp6v1b2 from the gills of P. annectens

Similar to F-ATPases, V-ATPases operate by a rotary mechanism (Imamura et al., 2003). Hydrolysis of ATP within the peripheral V_1 complex causes conformation changes in the A subunit, rotating the central rotary complex that includes a ring of proteolipid subunits within integral V_0 domain. Cytoplasmic H^+ enters the V_0 complex, binds to glutamic acid residues in the proteolipid ring, rotates together with the ring, and deprotonates by arginine before release through a hemi-channel into the lumen (review by Cipriano et al., 2008). In the V_1 domain, three A and B subunits are alternately arranged in a hexamer with nucleotide binding sites located at the interfaces. Although residues for the three catalytic sites are mainly contributed by the A subunits, the B subunits also contribute some residues to the catalytic sites and form most of the non-catalytic regulatory sites (Liu et al., 1996; MacLeod et al., 1998). As subunit B is always in the cytoplasm, Atp6v1b1 and Atp6v1b2 obtained from the gills of *P. annectens* did not consist of any transmembrane region based on the prediction by TOPCONS.

For yeast V-ATPase subunit B (Vma2p), Liu et al. (1996) demonstrated that mutations of amino acids in non-catalytic binding sites led to only moderate decreases in activity, but drastic reductions in activity were resulted from mutations of amino acids in the catalytic sites. For instance, two mutations at the catalytic sites, R381S (position 395 in Atp6v1b1 and 399 in Atp6v1b2 of *P. annectens*) and Y352S (position 366 in Atp6v1b1 and 370 in Atp6v1b2 of *P.*

annectens), completely prevented H^+ transport. The R381S mutation also affects the assembly of the V-ATPase, because R381 can act as a contact point between A and B subunits. As arginine carries a positive charge, R381 can also contribute to the stabilization of the transitional stage during ATP hydrolysis. For Atp6v1b1 of *P. annectens*, it could still be functional despite the replacement of tyrosine at residue 352 by phenylalanine, as Y352F mutation in yeast only leads to 20% reduction in activity (Liu et al., 1996).

Vha can form links with the cytoskeleton. At the N-terminus, both Atp6v1b1 and Atp6v1b2 of *P. annectens* possess a profilin-like domain (Chen et al., 2004) located within a microfilament binding site (Holliday et al., 2000). However, Atp6v1b1, but not Atp6v1b2, had a PDZ-binding domain D(S/T)XL near the C-terminus, indicating that it could bind with PDZ proteins such as the Na^+/H^+ exchanger regulatory factor (NHE-RF), which can in turn bind with actin-binding proteins (Breton et al., 2000). The differences between Atp6v1b1 and Atp6v1b2 concerning their interaction with the cytoskeleton can result in their distinct localization (apical and basolateral, respectively) in the gill of *P. annecten*.

4.3. Gills of P. annectens have high expression levels of atp6v1b1 and atp6v1b2

In *P. annectens*, the transcript levels of both *atp6v1b1* and *atp6v1b2* were generally higher in the gills than in other organs, indicating that Vha could serve some important branchial functions. It has been established that Vha is generally expressed in fish gills, and the excretion of H^+ through Vha promotes branchial ammonia excretion by trapping the excreted NH_3 as NH_4^+ (Nawata et al., 2007; Moreira-Silva et al., 2010). Although the skin of *P. annectens* also consists of ionocytes (Sturla et al., 2001a), the relatively low expression levels of *atp6v1b1* and the lack of *atp6v1b2* expression therein suggested that it played a relatively minor role in H^+ excretion through Vha. Of note, the giant mudskipper, *P. schlosseri*, can also reduce the ambient pH during exposure to an external medium containing ammonia or having high alkalinity (Ip et al., 2004c). The increased acid excretion occurs mainly in the head region of

P. schlosseri and is inhibited by bafilomycin A1 indicating the involvement of Vha (Ip et al. 2004c).

4.4. The apical and basolateral localization of Atp6v1b in two different types of ionocytes in the gills of P. annectens

Vha can be localized in the apical (Lin et al., 1994; Sullivan et al., 1995; Wilson et al., 1997, 2000b) or basolateral membrane of ionocytes in fish gills (Piermarini and Evans, 2000; Katoh et al., 2003; Tresguerres et al., 2007). In the gills of *P. annectens*, Atp6v1b that comprised both Atp6v1b1 and Atp6v1b2 was immunolocalized in two different types of Nka-immuno-reactive ionocytes, although not all Nka-immunoreactive cells were Atp6v1b-immunoreactive. Branchial epithelial cells that are immunoreactive to both Vha and Nka have been reported for another air-breathing fish, *Trichogaster microlepis* (Huang et al., 2010). For *P. annectens*, the apical and basolateral immunostaining of Atp6v1b in different ionocytes could be attributed to the distinct subcellular localization of Atp6v1b1 and Atp6v1b2. There was a PDZ-binding domain at the C-terminus of Atp6v1b1, but not Atp6v1b2, of *P. annectens*, and this domain could enable Atp6v1b1 to interact with NHE-RF, which in turn interacted with the cytoskeleton (Murthy et al., 1998; Breton et al., 2000). It has been postulated that this cytoskeleton interaction leads to the apical localisation of Atp6v1b1 in epithelial cells (Boesch et al., 2003a). For instance, Atp6v1b1 and Atp6v1b2 have an apical and a basolateral localization, respectively, in the epithelial cells of the swim bladder of the European eel, *Anguilla anguilla* (Boesch et al., 2003b). As the anti-Atp6v1b antibody used in this study detected both Atp6v1b1 and Atp6v1b2, it can explain why one type of ionocyte displayed apical immunolabeling while another type displayed basolateral immunolabeling in the gills of *P. annectens*. These two types of ionocyte are likely to have different physiological functions, and those displayed apical localization of Atp6v1b (probably Atp6v1b1) can probably transport H^+ to the external medium.

4.5. Ammonia-loading leads to increases in the branchial protein abundance of Atp6v1b and activity of Vha as well as the capacity to acidify the external medium in P. annectens

567 Under normal conditions, the excretion of H^+ through the branchial Vha would favor the
568 excretion of ammonia through Rhgps in *P. annectens* (Chng et al., 2017). Estivating *P.*
569 *annectens* can downregulated the gene and protein expression levels of *rhag*/Rhag, *rhbg*/Rhbg
570 and *rhcg*/Rhcg in its gills to impede ammonia excretion during the induction and maintenance
571 phases of aestivation but upregulated their expression levels during the arousal phase to regain
572 the ability of ammonia excretion (Chng et al., 2017). At present, it is uncertain whether the
573 expression levels of *rhgps*/Rhgps would be downregulated in the gills of *P. annectens*
574 confronted with ammonia-loading. Nonetheless, our results demonstrated that exposure to 100
575 mmol l^{-1} NH_4Cl for six days led to an increase in the activity of Vha in the gills of *P. annectens*.
576 Vha can be regulated at different levels, from transcriptional and translational regulation
577 to non-expressional regulation such as the assembly of the different subunits (review by Gluck
578 et al., 1996). The expression of Atp6v1b in the gills of *P. annectens* in response to ammonia-
579 loading conditions was regulated at the translational level, possibly because of the presence of
580 relatively high levels of *atp6v1b1*/*atp6v1b2* transcripts ($\times 10^4$ copies per ng total RNA) in the
581 gills of the control fish. At the transcript level, *atp6v1b1*/*atp6v1b2* responded differently during
582 ammonia exposure, but they were not augmented. By contrast, the integral protein abundance
583 of Atp6v1b increased significantly in the gills of *P. annectens* after six days of exposure to 100
584 mmol l^{-1} NH_4Cl, although the relative contribution of Atp6v1b1 and Atp6v1b2 to this increase
585 was unresolved. The upregulation of Atp6v1b expression by translation without involving
586 increased transcription could respond faster to external changes and avoid the energy
587 expenditure needed for the synthesis, processing and exporting of mRNA (Lackner and Bähler,
588 2008).
589 The increase in Atp6v1b protein abundance occurred in association with an increase in
590 the activity of Vha in the gills of *P. annectens*, indicating that ammonia exposure augmented
591 the capacity of Vha to transport H^+. In addition, individuals of *P. annectens* that had been
592 exposed to 100 mmol l^{-1} NH_4Cl for six days had a stronger capacity to lower the pH of the

external medium containing ammonia, indicating a greater capacity of acid excretion. Nonetheless, this cannot be regarded simply as a response to facilitate ammonia excretion as proposed previously for *O. mykiss* (Nawata et al., 2007) and *M. anguillicaudatus* (Moreira-Silva et al., 2010), which were exposed to relatively low concentrations of environmental ammonia. For *P. annectens* exposed to ammonia-loading conditions (100 mmol l^{-1} NH_4Cl), the increased capacity to lower the pH of the external medium (Fig. 8) could function primarily to decrease the proportion of [NH_3] to [NH_4^+] in the external medium (Fig. 9) in order to reduce the toxicity of environmental ammonia.

4.6. Relationships between environmental ammonia detoxification and increased urea synthesis in P. annectens exposed to ammonia-loading conditions

An important component of the OUC, carbamoyl phosphate synthetase III (CPS III), is expressed in the liver of African lungfishes (Chew et al., 2003b; Loong et al., 2005). When exposed to environmental ammonia, African lungfishes can increase the synthesis and excretion of urea to maintain the plasma ammonia at low concentrations (< 0.3 mmol l^{-1}) by (Chew et al., 2005; Loong et al., 2005, 2012). While the detoxification of ammonia to urea alleviates the internal organs, particularly the brain, from ammonia toxicity, the low ammonia concentration in the plasma can draw a large influx of NH_3 down an inwardly directed P_{NH3} gradient during ammonia-loading. As the detoxification of ammonia to urea is energy intensive, with 5 mol of ATP equivalent being hydrolysed for each mole of urea synthesized (Ip et al., 2001), the concurrent detoxification of endogenous and exogenous ammonia would result in high energy expenditure. Therefore, complementary strategies are needed to reduce the influx of exogenous ammonia in order to minimize the magnitude of increased urea synthesis during ammonia-loading (Chew et al., 2005). It has been reported that the skins of African lungfishes have relatively low NH_3 permeability (*P. dolloi*, Chew et al., 2005; *P. aethiopicus*, Loong et al., 2007). Importantly, the influx of NH_3 is further reduced by lowering the ambient pH through increased acid excretion, which can be regarded as a strategy of 'environmental ammonia

619 detoxification' (Chew et al., 2003a; Ip et al., 2004c; Wood et al., 2005). During ammonia-
620 loading, the increased expression of Atp6v1b and activity of Vha in the gills of *P. annectens*
621 could augment the capacity of acid excretion, rendering urea synthesis a feasible and effective
622 strategy to detoxify endogenous ammonia.

623 ***4.7. Conclusion***

624 Two gene isoforms of *Vha subunit B*, *atp6v1b1* and *atp6v1b2*, had been identified in the gills
625 of *P. annectens*, which shared homology with the kidney and brain isoforms, respectively, from
626 other species. The gene expression levels of *atp6v1b1* and *atp6v1b2* in the gills were high, and
627 Atp6v1b was localised to the apical or basolateral membranes of certain branchial epithelial
628 cells. Those cells with apical Atp6v1b (probably Atp6v1b1) could be responsible for H^+
629 excretion. After six days of exposure to 100 mmol l^{-1} NH_4Cl, the protein abundance of Atp6v1b
630 and the activity of Vha increased ~3-fold and ~2-fold, respectively, in the gills of *P. annectens*.
631 Furthermore, exposure to100 mmol l^{-1} NH_4Cl for six days increased in the ability of *P.*
632 *annectens* to lower the pH of the medium containing ammonia. Taken altogether, our results
633 indicate that the branchial Vha could be the transporter responsible for the increased acid
634 excretion in *P. annectens* confronted with ammonia-loading conditions. Acidifying the external
635 medium, in combination with a low ammonia permeability in the skin, is probably the most
636 effective strategy to defence against environmental ammonia toxicity, as ammonia
637 detoxification is conducted in the external medium prior to its infiltration into the fish's body.
638

Acknowledgements

This study was supported by the Singapore Ministry of Education through a grant (R154-000-429-112) administered to Y. K. Ip.

Conflict of interest

The authors declare that the research was conducted in the absence of any commercial or financial relationships that could be construed as a potential conflict of interest.

References

Boesch, S.T., Eller, B., Pelster, B., 2003a. Expression of two isoforms of the vacuolar-type ATPase subunit B in the zebrafish *Danio rerio*. J. Exp. Biol. 206, 1907-1915.

Boesch, S.T., Niederstätter, H., Pelster, B., 2003b. Localization of the vacuolar-type ATPase in swimbladder gas gland cells of the European eel (*Anguilla anguilla*). J. Exp. Biol. 206, 469-475.

Bradford, M.M., 1976. A rapid and sensitive method for quantitation of microgram quantities of protein utilizing the principle of protein-dye binding. Anal. Biochem. 72, 248-254.

Breton, S., Wiederhold, T., Marshansky, V., Nsumu, N.N., Ramesh, V., Brown, D., 2000. The B1 subunit of the H^+ ATPase is a PDZ domain-binding protein: colocalization with the NHE-RF in renal B-intercalated cells. J. Biol. Chem. 275, 18219-18224.

Brien, P., Poll, M., Bouillon, J., 1959. Ethologie de la reproduction de *Protopterus dolloi* Blgr. Ann. Mus. R. Congo Belg. Ser. 8, 71, 3–21.

Burggren, W.H., Johansen, K., 1986. Circulation and respiration in lungfishes (Dipnoi). J. Morphol. Suppl. 1, 217–236.

Chen, S.H., Bubb, M.R., Yarmola, E.G., Zuo, J., Jiang, J., Lee, B.S., Lu, M., Gluck, S.L., Hurst, I.R., Holliday, L.S., 2004. Vacuolar H^+-ATPase binding to microfilaments: regulation in response to phosphatidylinositol 3-kinase activity and detailed characterisation of the actin-binding site in subunit B. J. Biol. Chem. 279, 7988-7998.

Chew, S.F., Ching, B., Chng, Y.R., Ong, J.L.Y., Hiong, K.C., Chen, X.L., Ip, Y.K., 2015. Aestivation in African lungfishes: physiology, biochemistry and molecular biology. In Phylogeny, Anatomy and Physiology of Ancient Fishes (ed. Zaccone, G., Dabrowski, K., Hedrick, M.S., Fernandes, J.M.O., Icardo, J.M.) p. 81-132. CRC Press, Boca Raton, FL.

670 Chew, S.F., Hiong, K.C., Lam, S.P., Ong, S.W., Wee, W.L., Wong, W.P., Ip, Y.K., 2014.
671 Functional roles of Na^+/K^+-ATPase in active ammonia excretion and seawater
672 acclimation in the giant mudskipper, *Periophthalmodon schlosseri*. Front. Physiol. 5,
673 158.
674 Chew, S.F., Ho, L., Ong, T.F., Wong, W.P., Ip, Y.K., 2005. The African lungfish, *Protopterus*
675 *dolloi*, detoxifies ammonia to urea during environmental ammonia exposure. Physiol.
676 Biochem. Zool. 78, 31-39.
677 Chew, S.F., Hong, L.N., Wilson, J.M., Randall, D.J., Ip, Y.K., 2003a. Alkaline environmental
678 pH has no effect on ammonia excretion in the mudskipper *Periophthalmodon schlosseri*
679 but inhibits ammonia excretion in the related species *Boleophthalmus boddaerti*.
680 Physiol. Biochem. Zool. 76, 204-214.
681 Chew, S.F., Ip, Y.K., 2014. Excretory nitrogen metabolism and defence against ammonia
682 toxicity in air-breathing fishes. J. Fish Biol. 84, 603-638.
683 Chew, S.F., Ip, Y.K., 2017. Nitrogen metabolism and nitrogenous wastes excretion. In: Fish
684 Out of Water: The Biology and Ecology of Mudskippers (ed. Zeehan, J., Murdy, E.O.)
685 p. 167-194. CRC Press, Boca Raton, FL.
686 Chew, S.F., Ong, T.F., Ho, L., Tam, W.L., Loong, A.M., Hiong, K.C., Wong, W.P., Ip, Y.K.,
687 2003b. Urea synthesis in the African lungfish *Protopterus dolloi* - hepatic carbamoyl
688 phosphate synthetase III and glutamine synthetase can be up-regulated by 6 days of
689 aerial exposure. J. Exp. Biol. 206, 3615-3624.
690 Chew, S.F., Wilson, J.M., Ip, Y.K., Randall, D.J., 2006. Nitrogenous excretion and defense
691 against ammonia toxicity. Fish Physiol. 21, 307-395.
692 Chng, Y.R., Ong, J.L.Y., Ching, B., Chen, X.L., Hiong, K.C., Wong, W.P, Chew, S.F., Ip,
693 Y.K., 2017. Molecular characterization of three Rhesus glycoproteins from the gills of

694 the African lungfish, *Protopterus annectens*, and effects of aestivation on their mRNA
695 expression level and protein abundance. PloS one 12 (10), e0185814.
696 Chng, Y.R., Ong, J.L.Y., Ching, B., Chen, X.L., Hiong, K.C., Wong, W.P., Chew, S.F., Lam,
697 S.H., Ip, Y.K., 2016. Molecular Characterization of aquaporin 1 and aquaporin 3 from
698 the gills of the African Lungfish, *Protopterus annectens*, and changes in their branchial
699 mRNA expression levels and protein abundance during three phases of aestivation.
700 Front. Physiol. 7:532. doi: 10.3389/fphys.2016.00532.
701 Cipriano, D.J., Wang, Y., Bond, S., Hinton, A., Jefferies, K.C., Qi, J., Forgac, M., 2008.
702 Structure and regulation of the vacuolar ATPases. Biochim. Biophys. Acta 1777, 599-
703 604.
704 Evans, D.H., Piermarini, P.M., Choe, K.P., 2005. The multifunctional fish gill: dominant site
705 of gas exchange, osmoregulation, acid-base regulation, and excretion of nitrogenous
706 waste. Physiol. Rev. 85, 97-177.
707 Fishman, A.P., Pack A.I., Delaney, R.G., Galante, R.J., 1986. Estivation in *Protopterus*. J.
708 Morphol. Suppl. 190, 237-248.
709 Forgac, M., 2000. Structure, mechanism and regulation of the clathrin-coated vesicle and yeast
710 vacuolar H^+-ATPases. J. Exp. Biol. 203, 71-80.
711 Gluck, S.L., Underhill, D.M., Iyori, M., Holliday, L.S., Kostrominova, T.Y., Lee, B.S., 1996.
712 Physiology and biochemistry of the kidney vacuolar H^+-ATPase. Annu. Rev. Physiol.
713 58, 427-445.
714 Graham, J.B., 1997. Air-breathing fishes: evolution, diversity, and adaptation. Academic Press,
715 New York.
716 Hall, T.A., 1999. BioEdit: a user-friendly biological sequence alignment editor and analysis
717 program for Windows 95/98/NT. Nucl. Acids Symp. Ser. 41, 95-98.

718 Hillaby, B.A., Randall, D.J., 1979. Acute ammonia toxicity and ammonia excretion in rainbow
719 trout (*Salmo gairdneri*). J. Fish. Res. Board Can. 36, 621-629.

720 Holliday, L.S., Lu, M., Lee, B.S., Nelson, R.D., Solivan, S., Zhang, L., Gluck, S.L., 2000. The
721 amino-terminal domain of the subunit B of vacuolar H^+-ATPase contains a filamentous
722 actin binding site. J. Biol. Chem. 275, 32331-32337.

723 Huang, C.Y., Chao, P.L., Lin, H.C., 2010. Na^+/K^+-ATPase and vacuolar-type H^+-ATPase in
724 the gills of the aquatic air-breathing fish *Trichogaster microlepis* in response to salinity
725 variation. Comp. Biochem. Physiol. A Mol. Integr. Physiol. 155, 309-318.

726 Hwang, P.P., Lee, T.H., 2007. New insights into fish ion regulation and mitochondrion-rich
727 cells. Comp. Biochem. Physiol. A 148, 479–497.

728 Hwang, P.P., Lee, T.H., Lin, L.Y., 2011. Ion regulation in fish gills: recent progress in the
729 cellular and molecular mechanisms. Am. J. Physiol. Regul. Integr. Comp. Physiol. 301,
730 R28-R47.

731 Imamura, H., Nakano, M., Noji, H., Muneyuki, E., Ohkuma, S., Yoshida, M., Yokoyama, K.,
732 2003. Evidence for rotation of V_1-ATPase. Proc. Natl. Acad. Sci. USA 100, 2312-2315.

733 Ip, Y.K., Chew, S.F., 2010. Ammonia production, excretion, toxicity, and defense in fish: a
734 review. Front. Physiol. 1, 134.

735 Ip, Y.K., Chew, S.F., 2018. Air-breathing and excretory nitrogen metabolism in fishes. Acta
736 Histochem. 120, 680-690.

737 Ip, Y.K., Chew, S.F., Randall, D.J., 2001. Ammonia toxicity, tolerance, and excretion. Fish
738 Physiol. 20, 109-148.

739 Ip, Y.K., Chew, S.F., Randall, D.J., 2004a. Five tropical air-breathing fishes, six different
740 strategies to defend against ammonia toxicity on land. Physiol. Biochem. Zool. 77, 768-
741 782.

742 Ip, Y.K., Chew, S.F., Wilson, J.M., Randall, D.J., 2004b. Defences against ammonia toxicity
743 in tropical air-breathing fishes exposed to high concentrations of environmental
744 ammonia: a review. J. Comp. Physiol. B 174, 565-575.

745 Ip, Y.K., Ching, B., Hiong, K.C., Choo, C.Y.L., Boo, M.V., Wong, W.P., Chew, S.F., 2015.
746 Light induces changes in activities of Na^+/K^+-ATPase, H^+/K^+-ATPase and glutamine
747 synthetase in tissues involved directly or indirectly in light-enhanced calcification in
748 the giant clam, *Tridacna squamosa*. Front. Physiol. 6:68. doi:
749 10.3389/fphys.2015.00068.

750 Ip, Y.K., Randall, D.J., Kok, T.K., Barzaghi, C., Wright, P.A., Ballantyne, J.S., Wilson, J.M.,
751 Chew, S.F., 2004c. The giant mudskipper *Periophthalmodon schlosseri* facilitates
752 active NH_4^+ excretion by increasing acid excretion and decreasing NH_3 permeability in
753 the skin. J. Exp. Biol. 207, 787-801.

754 IUCN, 2021. The IUCN Red List of Threatened Species. Version 2021-3.

755 Jones, D.T., Taylor, W.R., Thornton, J.M., 1992. The rapid generation of mutation data
756 matrices from protein sequences. Comput. Appl. Biosci. 8, 275-282.

757 Katoh, F., Hyodo, S., Kaneko, T., 2003. Vacuolar-type proton pump in the basolateral plasma
758 membrane energizes ion uptake in branchial mitochondria-rich cells of killifish
759 *Fundulus heteroclitus*, adapted to a low ion environment. J. Exp. Biol. 206, 793-803.

760 Keane, T.M., Creevey, C.J., Pentony, M.M., Naughton, T.J., McInerney, J.O., 2006.
761 Assessment of methods for amino acid matrix selection and their use on empirical
762 data shows that ad hoc assumptions for choice of matrix are not justified. BMC Evol.
763 Biol. 6, 29.

764 Kirschner, L.B., 2004. The mechanism of sodium chloride uptake in hyperregulating aquatic
765 animals. J. Exp. Biol. 207, 1439-1452.

766 Lackner, D.H., Bähler, J., 2008. Translational control of gene expression: from transcripts to
767 transcriptomes. Int. Rev. Cell Mol. Biol. 271, 199-251.

768 Laemmli, U.K., 1970. Cleavage of structural proteins during the assembly of the head
769 bacteriophage T4. Nature 227, 680-685.

770 Lenfant, C., Johansen, K., 1968. Respiration in the African lungfish *Protopterus aethiopicus*.
771 1. Respiratory properties of blood and normal patterns of breathing and gas exchange.
772 J. Exp. Biol. **49**, 437–452.

773 Lim, C.K., Wong, W.P., Lee, S.M., Chew, S.F., Ip, Y.K., 2004. The ammonotelic African
774 lungfish *Protopterus dolloi* increases the rate of urea synthesis and becomes ureotelic
775 after feeding. J. Comp. Physiol. B 174, 555-564.

776 Lin, H., Pfeiffer, D., Vogl, A., Pan, J., Randall, D., 1994. Immunolocalization of H^+-ATPase
777 in the gill epithelia of rainbow trout. J. Exp. Biol. 195, 169-183.

778 Lin, H., Randall, D.J., 1991. Evidence for the presence of an electrogenic proton pump on the
779 trout gill epithelium. J. Exp. Biol. 161, 119-134.

780 Liu, Q., Kane, P.M., Newman, P.R., Forgac, M., 1996. Site-directed mutagenesis of the yeast
781 V-ATPase subunit B (Vma2p). J. Biol. Chem. 271, 2018-2022.

782 Liu, S.T., Tsung, L., Horng, J.L., Lin, L.Y., 2013. Proton-facilitated ammonia excretion by
783 ionocytes of medaka (*Oryzias latipes*) acclimated to seawater. Am. J. Physiol. Regul.
784 Integr. Comp. Physiol. 305, R242–R251.

785 Loong, A.M., Chng, Y.R., Chew, S.F., Wong, W.P., Ip, Y.K., 2012. Molecular characterization
786 and mRNA expression of carbamoyl phosphate synthetase III in the liver of the African
787 lungfish, *Protopterus annectens*, during aestivation or exposure to ammonia. J. Comp.
788 Physiol. B 182, 367-379.

789 Loong, A.M., Hiong, K.C., Lee, S.M., Wong, W.P., Chew, S.F., Ip, Y.K., 2005. Ornithine-urea
790 cycle and urea synthesis in African lungfishes, *Protopterus aethiopicus* and *Protopterus*
791 *annectens*, exposed to terrestrial conditions for six days. J. Exp. Zool. A 303, 354-365.

792 Loong, A.M., Tan, J.Y., Wong, W.P., Chew, S.F., Ip, Y.K., 2007. Defense against
793 environmental ammonia toxicity in the African lungfish, *Protopterus aethiopicus*:
794 bimodal breathing, skin ammonia permeability and urea synthesis. Aquat. Toxicol. 85,
795 76-86.

796 MacLeod, K.J., Vasilyeva, E., Baleja, J.D., Forgac, M., 1998. Mutational analysis of the
797 nucleotide binding sites of the yeast vacuolar proton-translocating ATPase. J. Biol.
798 Chem. 273, 150-156.

799 McMahon, B.R., 1970. The relative efficiency of gaseous exchange across the lungs and gills
800 of an African lungfish *Protopterus aethiopicus*. J. Exp. Biol. 52, 1–15.

801 Mindell, J.A., 2012. Lysosomal acidification mechanisms. Annu. Rev. Physiol. 74, 69-86.

802 Moreira-Silva, J., Tsui, T.K., Coimbra, J., Vijayan, M.M., Ip, Y.K., Wilson, J.M., 2010.
803 Branchial ammonia excretion in the Asian weatherloach *Misgurnus anguillicaudatus*.
804 Comp. Biochem. Physiol. C Toxicol. Pharmacol. 151, 40-50.

805 Murthy, A., Gonzalez-Agosti, C., Cordero, E., Pinney, D., Candia, C., Solomon, F., Gusella,
806 F., Ramesh, V., 1998. NHE-RF, a regulatory cofactor for Na^+-H^+ exchange, is a
807 common interactor for merlin and ERM (MERM) proteins. J. Biol. Chem. 273, 1273-
808 1276.

809 Nawata, C.M., Hung, C.C., Tsui, T.K., Wilson, J.M., Wright, P.A., Wood, C.M., 2007.
810 Ammonia excretion in rainbow trout (*Oncorhynchus mykiss*): evidence for Rh
811 glycoprotein and H^+-ATPase involvement. Physiol. Genomics 31, 463-474.

812 Nelson, R.D., Guo, X.L., Masood, K., Brown, D., Kalkbrenner, M., Gluck, S., 1992. Selectively
813 amplified expression of an isoform of the vacuolar H^+-ATPase 56-kilodalton subunit in
814 renal intercalated cells. Proc. Natl. Acad. Sci. USA 89, 3541-3545.

815 Perry, S.F., Shahsavarani, A., Georgalis, T., Bayaa, M., Furimsky, M., Thomas, S.L., 2003.
816 Channels, pumps, and exchangers in the gill and kidney of freshwater fishes: their role
817 in ionic and acid–base regulation. J. Exp. Zool. A 300, 53-62.

818 Piermarini, P.M., Evans, D.H., 2000. Effects of environmental salinity on Na(+)/K(+)-ATPase
819 in the gills and rectal gland of a euryhaline elasmobranch (*Dasyatis sabina*). J. Exp.
820 Biol. 2000 Oct;203(Pt 19), 2957-2966. doi: 10.1242/jeb.203.19.2957.

821 Randall, D.J., Wilson, J.M., Peng, K.W., Kok, T.W.K., Kuah, S.S.L., Chew, S.F., Lam, T.J.,
822 Ip, Y.K., 1999. The mudskipper, *Periophthalmodon schlosseri*, actively transports
823 NH_4^+ against a concentration gradient. Am. J. Physiol. **46,** R1562–R1567.

824 Seidelin, M., Brauner, C.J., Jensen, F.B., Madsen, S.S., 2001. Vacuolar-type H^+-ATPase and
825 Na^+, K^+-ATPase expression in gills of Atlantic salmon (*Salmo salar*) during isolated
826 and combined exposure to hyperoxia and hypercapnia in fresh water. Zool. Sci. 18,
827 1199-1206.

828 Shih, T.H., Horng, J.L., Hwang, P.P., Lin, L.Y., 2008. Ammonia excretion by the skin of
829 zebrafish (*Danio rerio*) larvae. Am. J. Physiol. Cell Physiol. 295, C1625-C1632.

830 Stamatakis, A., 2014. RAxML version 8: a tool for phylogenetic analysis and post-analysis
831 of large phylogenies. Bioinformatics 30, 1312-1313.

832 Sturla, M., Masini, M. A., Prato, P., Grattarola, C., Uva, B., 2001a. Mitochondria-rich cells in
833 gills and skin of an African lungfish, Protopterus annectens. Cell Tissue Res. 303, 341-
834 358.

835 Sturla, M., Prato, P., Grattarola, C., Masini, M. A., Uva, B., 2001b. Effects of induced
836 aestivation in *Protopterus annectens*: A histomorphological study. J. Exp. Zool. 292,
837 26-31.

838 Sullivan, G.V., Fryer, J.N., Perry, S.F., 1995. Immunolocalization of proton pumps (H^+-
839 ATPase) in pavement cells of rainbow trout gill. J. Exp. Biol. 198, 2619-2629.

840 Tomashek, J.J., Brusilow, W.S., 2000. Stoichiometry of energy coupling by proton-
841 translocating ATPases: a history of variability. J. Bioenerg. Biomembr. 32, 493-500.

842 Tresguerres, M., Parks, S.K., Wood, C.M., Goss, G.G., 2007. V-H^+-ATPase translocation
843 during blood alkalosis in dogfish gills: interaction with carbonic anhydrase and
844 involvement in the post-feeding alkaline tide. Am. J. Physiol. 292, R2012-R2019.

845 Tsirigos, K.D., Peters, C., Shu, N., Käll, L., Elofsson, A., 2015. The TOPCONS web server for
846 combined membrane protein topology and signal peptide prediction. Nucleic Acids Res.
847 43, W401-W407.

848 Ura, K., Soyano, K., Omoto, N., Adachi, S., Yamauchi, K., 1996. Localization of Na^+, K^+-
849 ATPase in tissues of rabbit and teleosts using an antiserum directed against a partial
850 sequence of the α-subunit. Zool. Sci. 13, 219-227.

851 van Hille, B., Richener, H., Schmid, P., Puettner, I., Green, J.R., Bilbe, G., 1994. Heterogeneity
852 of vacuolar H^+-ATPase: differential expression of two human subunit B isoforms.
853 Biochem. J. 303, 191-198.

854 Whitfield, M., 1974. The hydrolysis of ammonia ions in sea water - a theoretical study. J. Mar.
855 Biol. Assoc. UK 54, 565-580.

856 Wilkie, M.P., 1997. Mechanisms of ammonia excretion across fish gills. Comp. Biochem.
857 Physiol. A Physiol. 118, 39-50.

858 Wilson, J.M., Laurent, P., Tufts, B.L., Benos, D.J., Donowitz, M., Vogl, A.W., Randall, D.J.,
859 2000a. NaCl uptake by the branchial epithelium in freshwater teleost fish: an
860 immunological approach to ion-transport protein localization. J. Exp. Biol. 203, 2279 -
861 2296.

862 Wilson, J.M., Randall, D.J., Donowitz, M., Vogl, A.W., Ip, A.K., 2000b. Immunolocalization
863 of ion-transport proteins to branchial epithelium mitochondria-rich cells in the
864 mudskipper (*Periophthalmodon schlosseri*). J. Exp. Biol. 203, 2297-2310.

865 Wilson, J.M., Randall, D.J., Vogl, A.W., Iwama, G.K., 1997. Immunolocalization of proton-
866 ATPase in the gills of the elasmobranch, *Squalus acanthias*. J. Exp. Zool. 278, 78-86.

867 Wood, C.M., Walsh, P.J., Chew, S.F., Ip, Y.K., 2005. Ammonia tolerance in the slender
868 lungfish (*Protopterus dolloi*): the importance of environmental acidification. Can. J.
869 Zool. 83, 507-517.

870

Supplementary Table S1. GenBank accession numbers of Vacuolar-type H^+-ATPase B subunit of animals selected for phenogramic analysis.

	Animal species (GenBank accession no.)
Atp6v1b1/ATP6V1B1	*Chelonia mydas* ATP6V1B1 (**XP_007064072.1**)
	Python bivittatus ATP6V1B1 (**XP_007430892.1**)
	Pogona vitticeps ATP6V1B1 (**XP_020650854.1**)
	Alligator sinensis ATP6V1B1 (**XP_006031698.1**)
	Xenopus tropicalis Atp6v1b1 (**NP_001107734.1**)
	Lepisosteus oculatus Atp6v1b1 isoform X1 (**XP_006629187.1**)
	Lepisosteus oculatus Atp6v1b1 isoform X2 (**XP_015199285.1**)
Atp6v1b2/ATP6V1B2	*Periophthalmodon schlosseri* Atp6v1b2 (**AML22893.1**)
	Chelonia mydas ATP6V1B2 (**XP_007066373.1**)
	Chrysemys picta bellii ATP6V1B2 (**XP_005285142.1**)
	Python bivittatus ATP6V1B2 (**XP_007433795.1**)
	Pogona vitticeps ATP6V1B2 (**XP_020667978.1**)
	Xenopus tropicalis Atp6v1b2 (**NP_001072182.1**)
	Fundulus heteroclitus Atp6v1b2 (**XP_012716151.1**)
	Boleophthalmus pectinirostris Atp6v1b2 (**XP_020790301.1**)
	Anabas testudineus Atp6v1b2 (**XP_026212137.1**)
	Nanorana parkeri Atp6v1b2 (**XP_018421706.1**)
ATP6V1B	*Acanthaster planci* ATP6V1B (**XP_022091650.1**)

Legends to figures

Fig. 1. Alignment of the amino acid sequences of Vacuolar-type H^+-ATPase (Vha) subunit B1 (Atp6v1b1) and Vha subunit B2 (Atp6v1b2) from the gills of *Protopterus annectens* with ATP6V1B1 from *Bos taurus* (NP_788827.1), Atp6v1b2 from *Fundulus heteroclitus* (XP_012716151.1) and Vha subunit B (VMA2) from *Saccharomyces cerevisiae* (P16140.2). Shaded residues indicate identical or similar amino acids. Boxed residues indicate domains involved in binding to microfilaments (profilin-like) or PDZ proteins (PDZ). "P-loop" refers to the region corresponding to a glycine-rich loop in subunit A. Double underlined residues indicate a motif found in Vha subunit B. Asterisks indicate residues that contribute to catalytic sites on subunit A and diamonds indicate those involved in non-catalytic sites.

Fig. 2. Phenogramic analysis of Vacuolar-type H^+-ATPase (Vha) subunit B1 (Atp6v1b1) and Vha subunit B2 (Atp6v1b2) from the gills of *Protopterus annectens*, with other Atp6v1b1/ATP6V1B1 and Atp6v1b2/ATP6V1B2 sequences from selected animal species. Numbers presented at each branch point represent bootstrap percentage from 4000 replicates. Vha subunit B of the echinoderm *Acanthaster planci* is the outgroup.

Fig 3. Gene expression levels, expressed as transcript levels ($\times 10^4$ copies of transcript per ng total RNA) of *Vacuolar-type H^+-ATPase* (*Vha*) *subunit B1* (*atp6v1b1*; open bar) and *Vha subunit B2* (*atp6v1b2*; closed bar), in various organs of *Protopterus annectens* kept in fresh water.

Fig. 4. Immunofluorescence localization of Na^+/K^+-ATPase alpha-subunit (Nkaα) and Vacuolar-type H^+-ATPase (Vha) subunit B (Atp6v1b) in the gills of *Protopterus annectens*. (A) Differential interference contrast (DIC) image showing the structure of the gill lamellae (GL). (B) Immunostaining of Atp6v1b in green. (C) Immunostaining of Nkaα in mitochondria-rich (MR) cells in red. (D) Merged image of DIC, red channel

(Nkaα) and green channel (Atp6v1b) with a magnified inset showing the basolateral and apparent cytoplasmic localization of Nkaα display in many lamellar MR cells, and the probable apical staining (arrowheads) and basolateral staining (open arrowheads) of Atp6v1b in two different types of MR cells. Scale bar: 20 μm.

Fig. 5. Transcript levels ($\times 10^4$ copies of transcript per ng total RNA) of *Vacuolar-type H^+-ATPase* (*Vha*) *subunit B1* (*atp6v1b1*; open bar) or *Vha subunit B2* (*atp6v1b2*; closed bar) in the gills of *Protopterus annectens*. Individuals of *P. annectens* were kept in fresh water (FW; control) or exposed to 100 mmol l^{-1} NH_4Cl for 1 day (d), 3 d or 6 d. Results are presented as mean ± SEM (n = 5). Means not sharing the same letters for each gene are significantly different from each other (p-value < 0.05).

Fig. 6. Protein abundance of Vacuolar-type H^+-ATPase (Vha) subunit B (Atp6v1b) in the gills of *Protopterus annectens* kept in fresh water (FW; control) or exposed to 100 mmol l^{-1} NH_4Cl for six days. (A) A representative immunoblot of Atp6v1b, with tubulin as the reference protein. (B) Quantification of the protein abundance of Atp6v1b expressed arbitrarily as the ratio of the optical density of the Atp6v1b band to the optical density of the tubulin band. Results are presented as mean ± SEM (n = 4). *Significantly different from the control (p-value < 0.05).

Fig. 7. Bafilomycin-sensitive Vacuolar-type H^+-ATPase (Vha) activity (μmol Pi released min^{-1} g^{-1} tissue or μmol Pi released min^{-1} mg^{-1} protein) from the gills of *Protopterus annectens* kept in fresh water without NH_4Cl (control) or exposed to 100 mmol l^{-1} NH_4Cl for six days. *Significantly different from the value obtained for the control fish without prior exposure to 100 mmol l^{-1} NH_4Cl.

Fig. 8. Effects of exposure to ammonia-loading conditions on the capacity of *Protopterus annectens* to lower the pH of the ambient fresh water containing 100 mmol l^{-1} NH_4Cl (pH 7.0) with continuous aeration, as demonstrated by changes in the pH of the external medium through a 12-h period. The medium containing 100 mmol l^{-1} NH_4Cl without fish

928 acted as a blank (n = 4; closed square). The ammonia-containing medium could include
929 an individual of *P. annectens* that had no prior exposure to NH_4Cl (day 0; n = 4; closed
930 circle), or an individual that had been exposed to 100 mmol l^{-1} NH_4Cl for six days (day
931 6; n = 4; closed triangle). Results are presented as mean ± SEM. *Significantly different
932 from the value obtained for the control fish without prior exposure to 100 mmol l^{-1} NH_4Cl.
933 **Fig. 9.** An estimation of the concentration of NH_3 in the external medium containing 100 mM
934 of total ammonia using the Henderson-Hasselbalch equation NH_4Cl at each time point
935 (with reference to Fig. 8) based on the measured pH and a p*K* value of 9.25. The medium
936 containing 100 mmol l^{-1} NH_4Cl without fish acted as a blank (n = 4; closed square). The
937 ammonia-containing medium could include an individual of *P. annectens* that had no
938 prior exposure to NH_4Cl (day 0; n = 4; closed circle), or an individual that had been
939 exposed to 100 mmol l^{-1} NH_4Cl for six days (day 6; n = 4; closed triangle).
940

941

Fig. 1

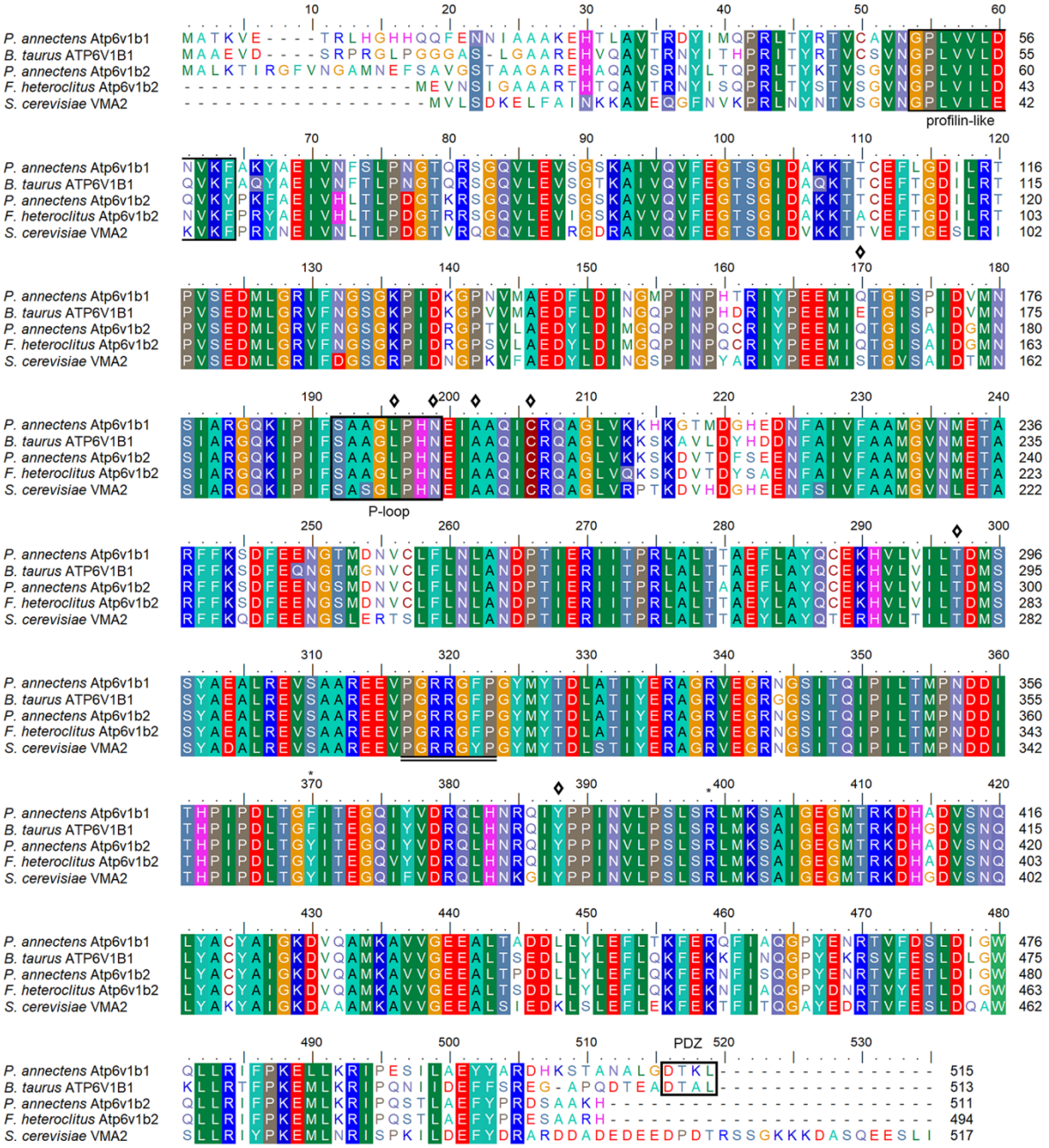

942

943

944

Fig. 2

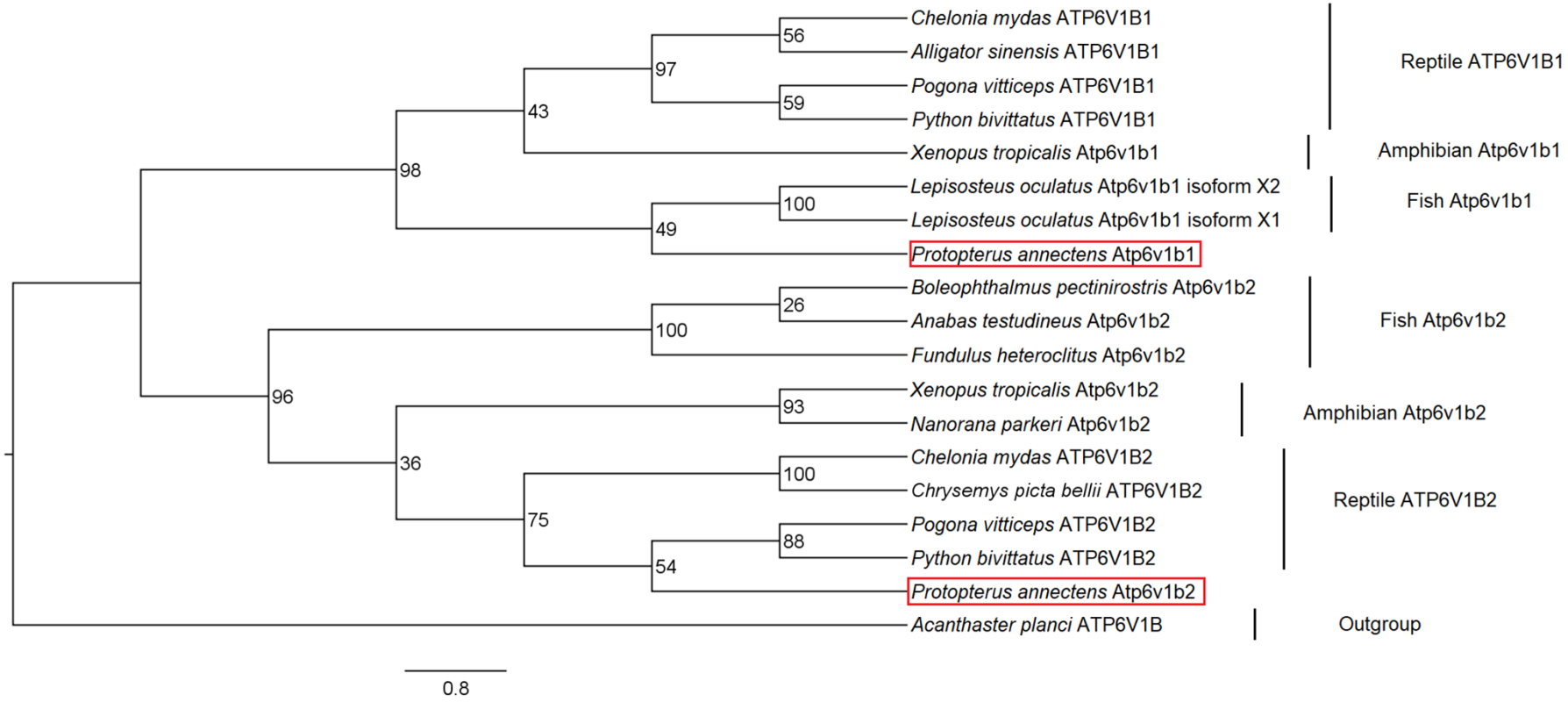

945

946

947

948

Fig. 3

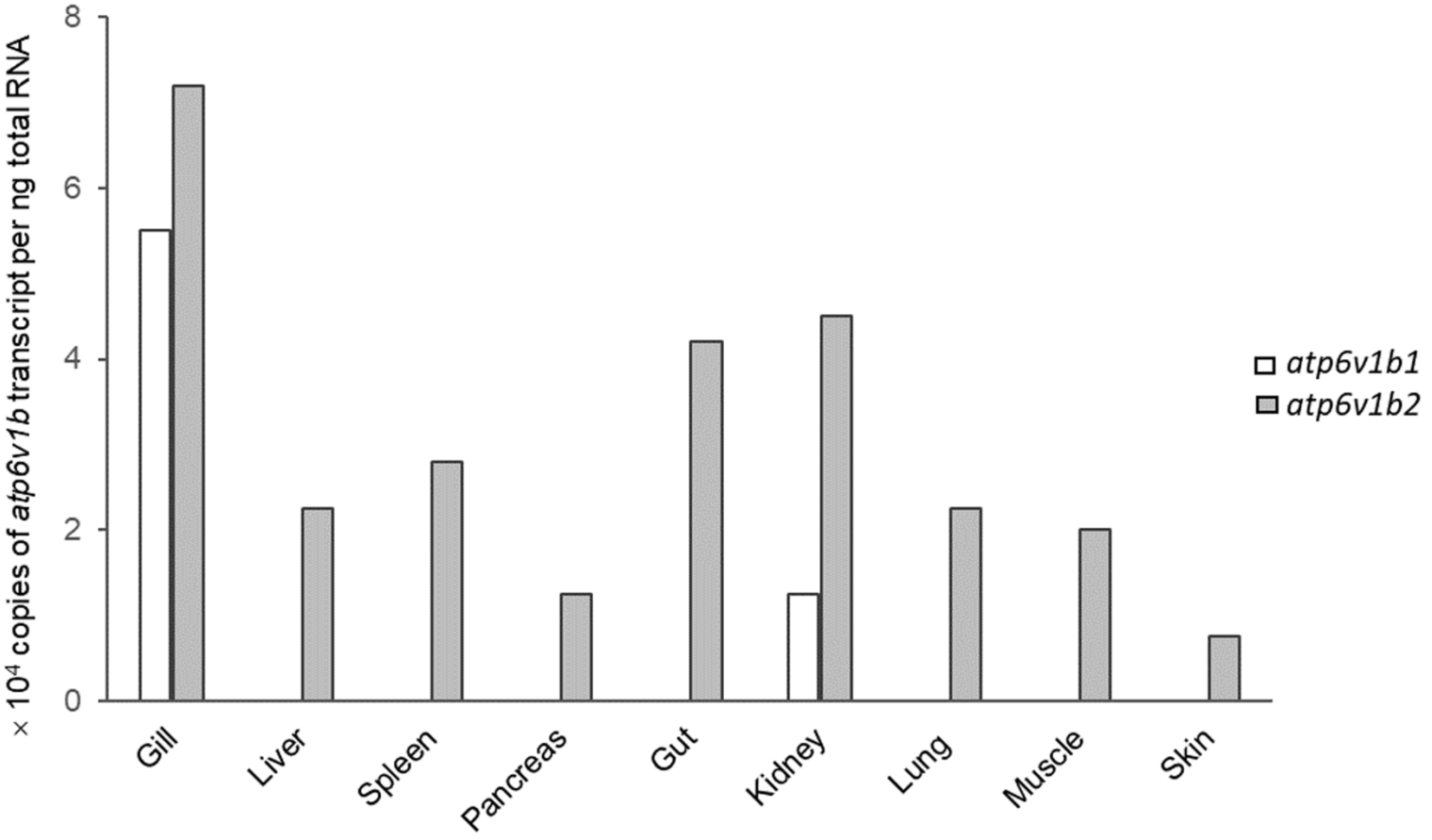

949

950

951

Fig. 4

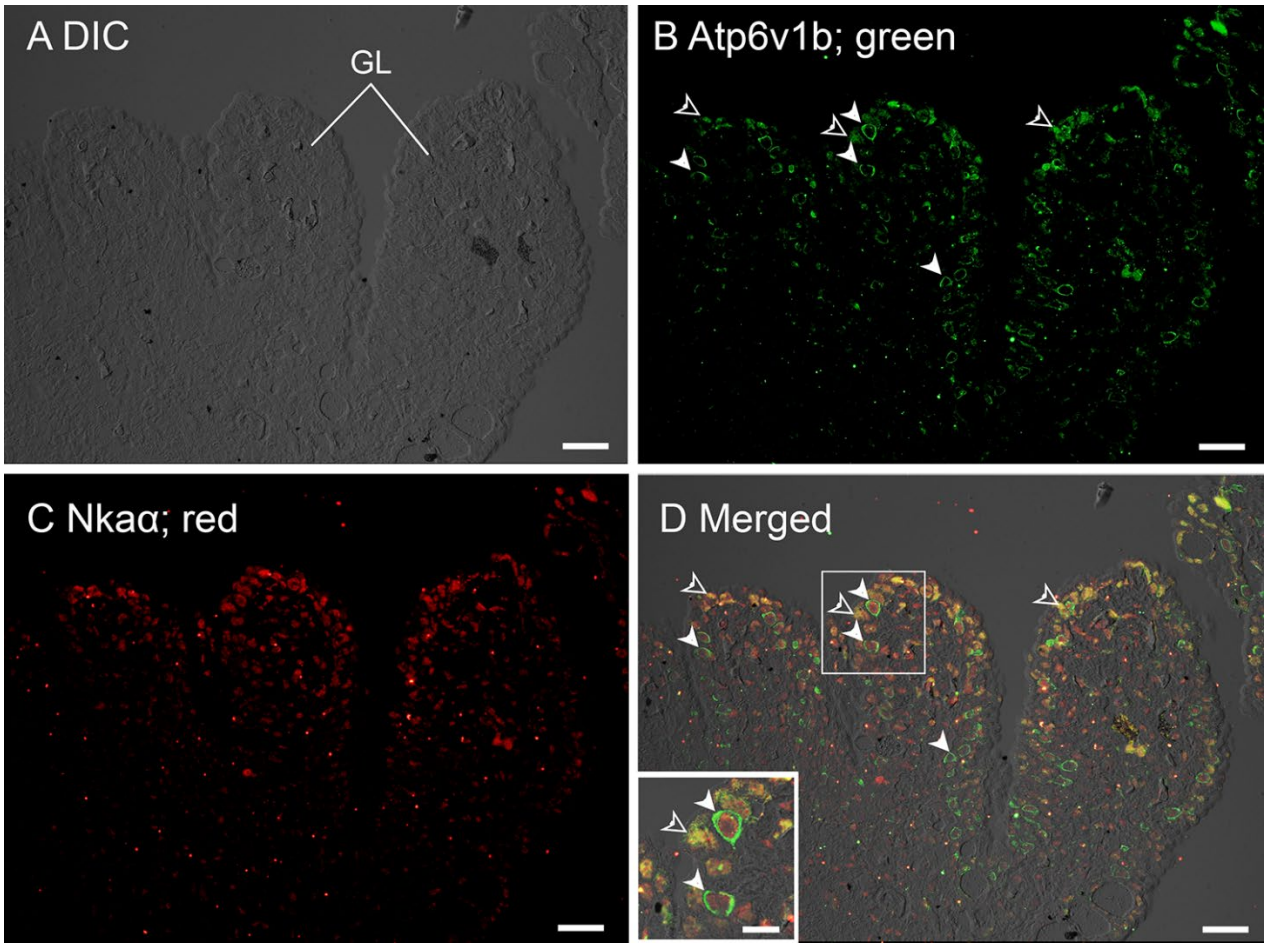

952

953

954

Fig. 5

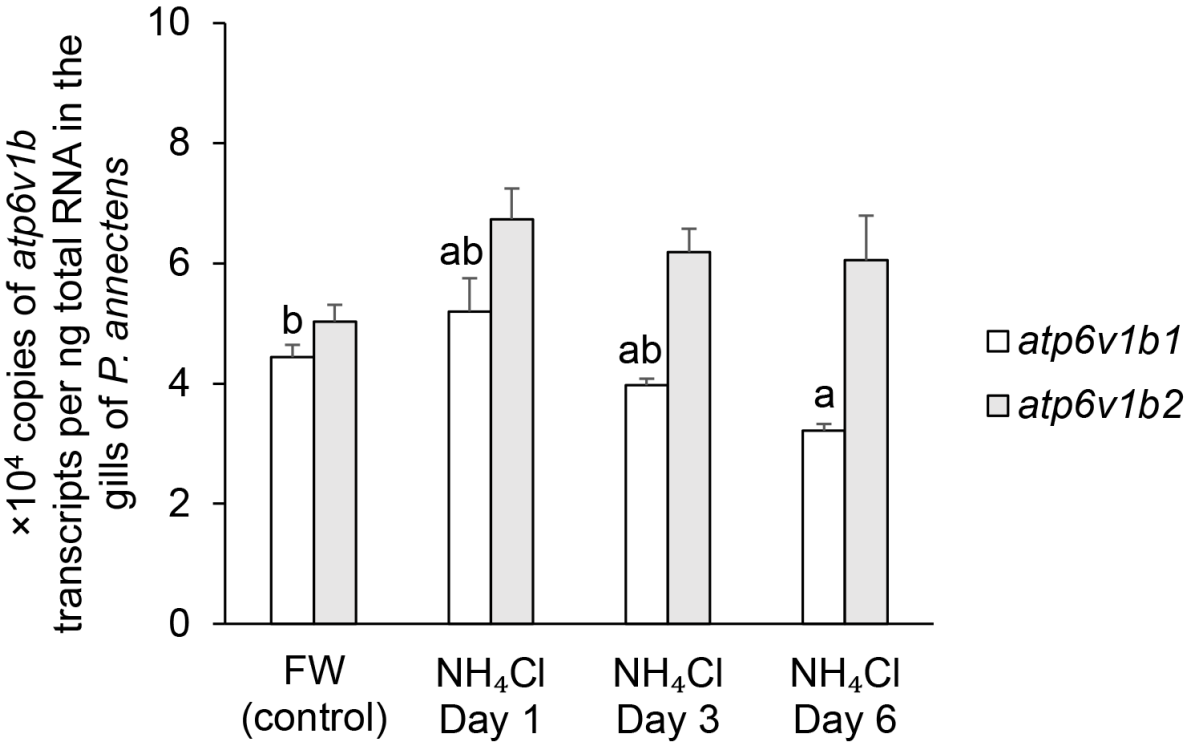

955

956

957

958

Fig. 6

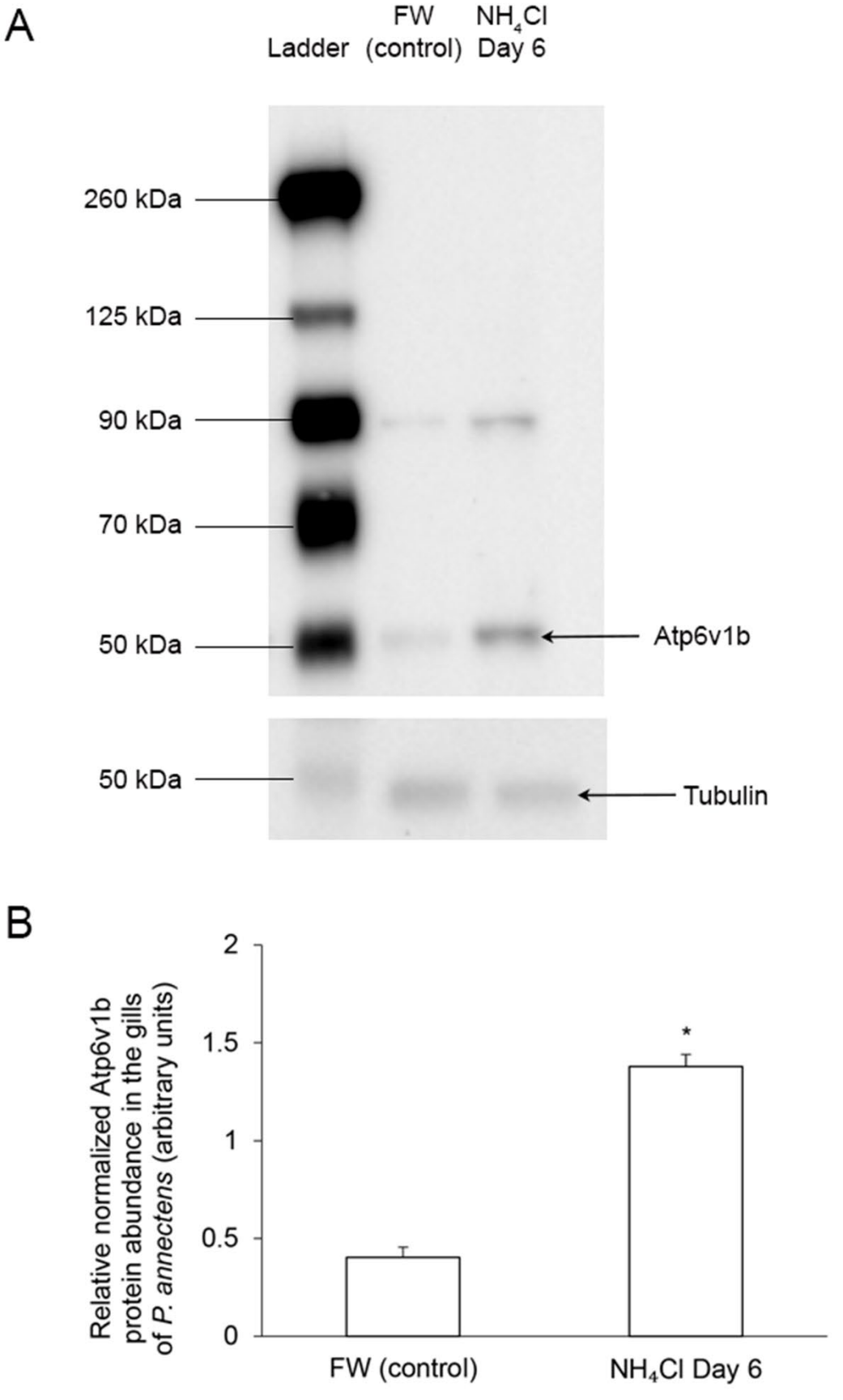
A
Ladder
FW (control)
NH4Cl Day 6
260 kDa
125 kDa
90 kDa
70 kDa
50 kDa
Atp6v1b
50 kDa
Tubulin
B
Relative normalized Atp6v1b protein abundance in the gills of P. annectens (arbitrary units)
2
1.5
1
0.5
0
*
FW (control)
NH4Cl Day 6

959

960 Fig. 7

961

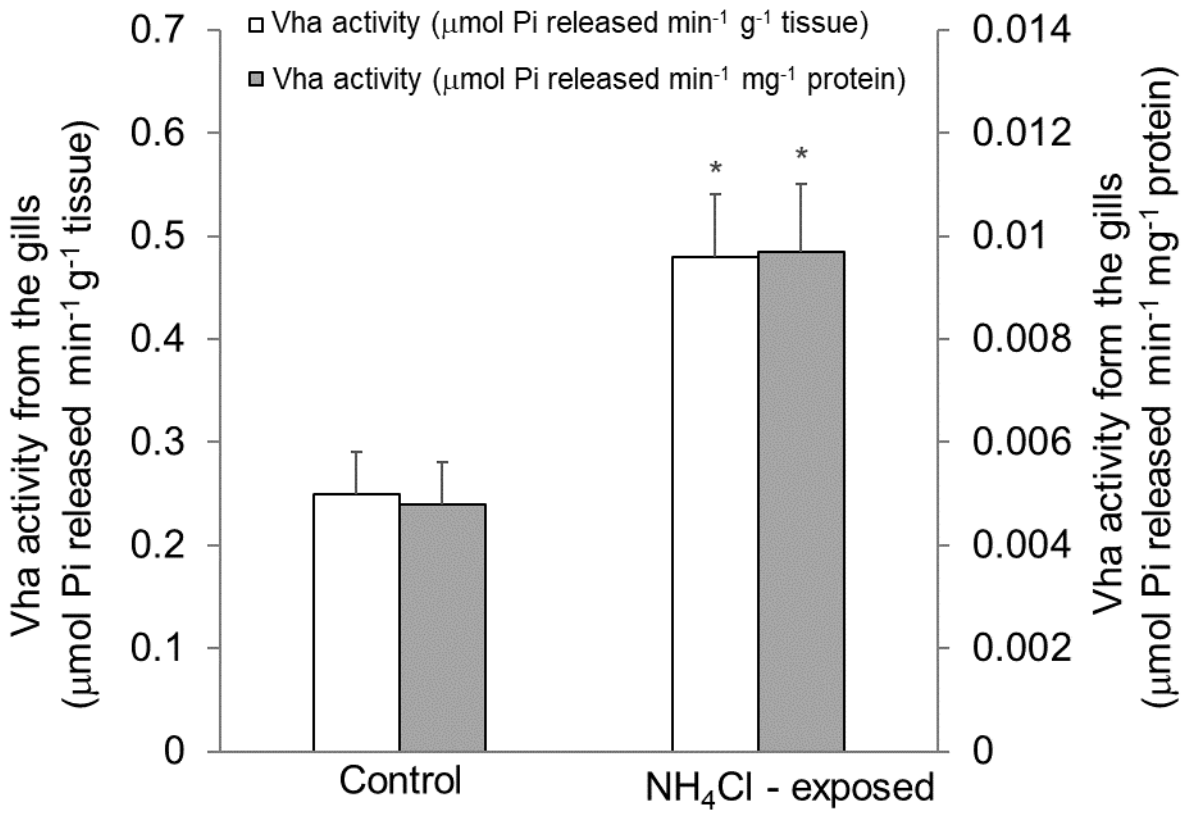

962

963

964

965

966

Fig. 8

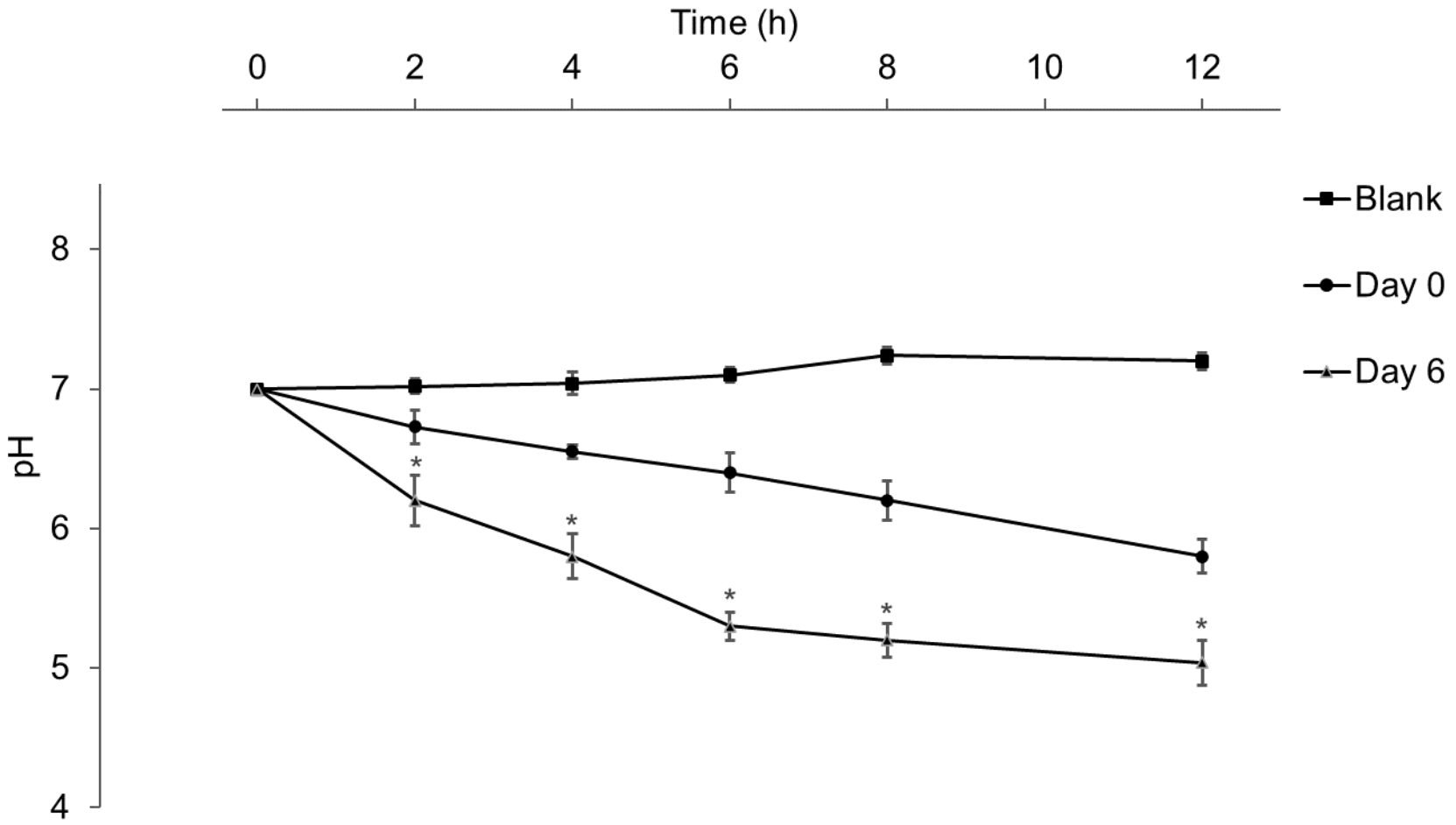

Fig. 9

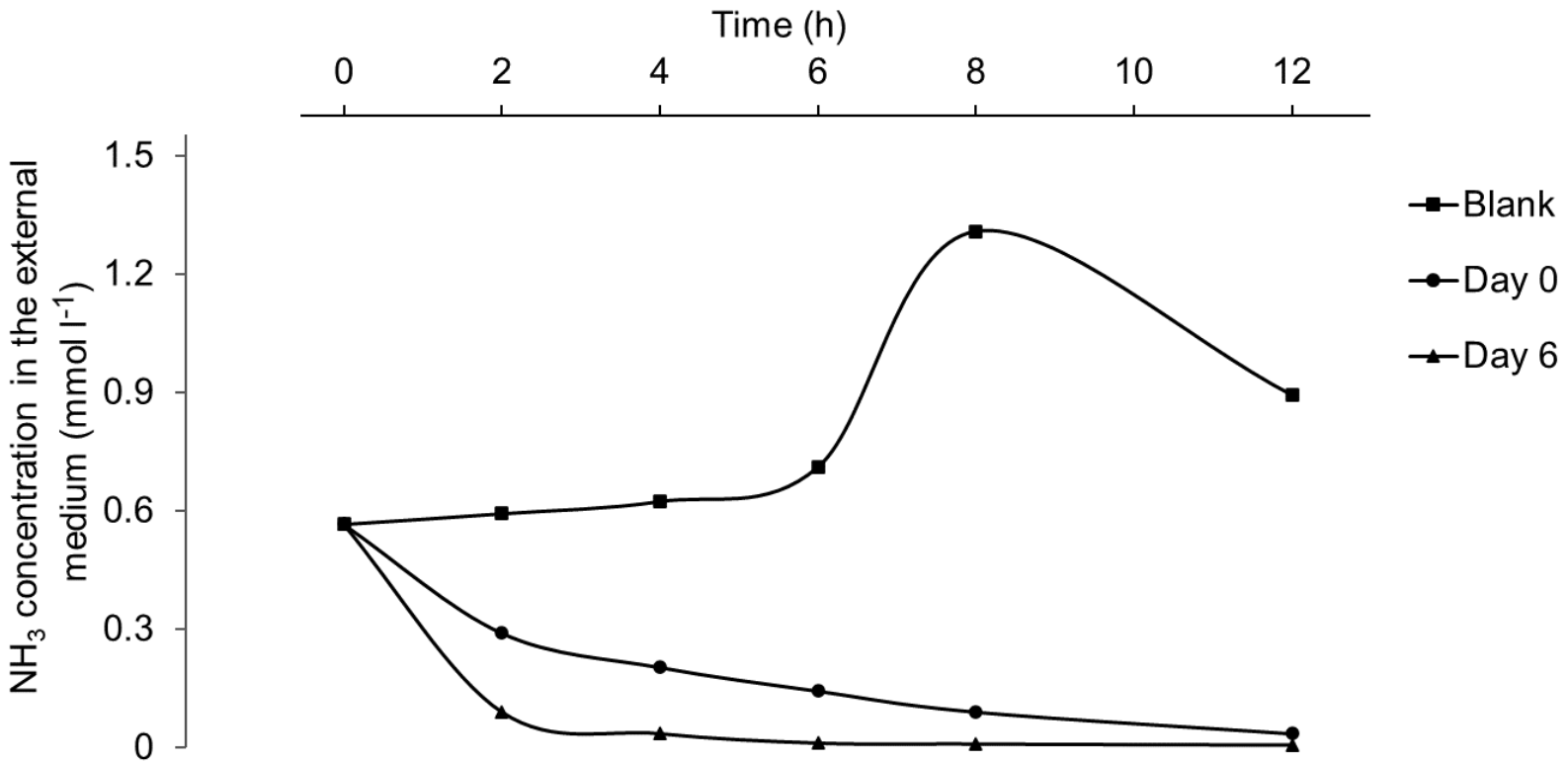
Time (h)
0
2
4
6
8
10
12
1.5
1.2
0.9
0.6
0.3
0
NH3 concentration in the external medium (mmol l-1)
Blank
Day 0
Day 6